The Abdus Salam International Centre for Theoretical Physics

IAEA International Atomic Energy Agency

unesco United Nations Educational, Scientific and Cultural Organization

12th AAMP Meeting & EFOMP School | (SMR 4071)

21 May 2025 - 24 May 2025
ICTP, Trieste, Italy

T01 - ANDROCKI Andrea

Comparison of DLG values obtained with five different measurement setups

T02 - BEGUS Ursa

Dosimetry from a Series of Whole-Body Planar Images and One SPECT/CT in Patients Undergoing Radionuclide Therapy using 177Lu-labelled Radiopharmaceuticals

T03 - BEN HAMMOUDA Farah

The need for standardization of geometrical feature computation for dose prevision models in radiotherapy

T04 - BITO Katarina

Calculation of electron mass stopping power in the range 0.01-1000 MeV in different human tissues

T05 - BONE Thomas Georg

Evaluation of Patient-Specific Quality Assurance Software Mobius3D and VeriQA in Comparison to the Eclipse Treatment Planning System

T06 - CHERIT HERNANDEZ Ariadna

Workflow and Planning Techniques for Stereotactic Ion Beam Therapy in Treating Cardiac Arrhythmias

T07 - DOVIJARSKI STANKIN Suzana

Dosimetry analysis of different planning techniques of whole breast radiotherapy

T08 - DUNDARA DEBELJUH Dea

The Defect Perfusion Index: A New Descriptor for the Characterization of Myocardial Perfusion Imaging Systems

T09 - FERNANDEZ RODRIGUEZ Alfredo

Towards optimized prescription metrics in novel radiotherapy techniques: A Machine Learning-guided study.

T10 - FERRARA Alessandro Michele

Ionoacoustic Dosimetry: Computational Simulations for Acoustic Detection of Proton and FLASH Electron Beams

T11 - FORGÁCS Csenge

Experiences with microcontroller-supported DAP measurements

T12 - FORNASIER Maria Rosa

Optimization of a quantitative SPECT/CT reconstruction protocol: phantom measurements and preliminary clinical evaluation.

T13 - GOLABOSKA Elena

Estimation of fetal dose during head and neck radiotherapy: Comparing IMRT and VMAT techniques for iX and Halcyon radiation units

T14 - JENSTERLE Luka

Challenges in introducing LUTATHERA to clinical practice

T15 - JUHASZ KOLLAR Nandor Attila

This study verifies MLC DLG and transmission values for Varian Clinac iX and TrueBeam using dose leakage measurements. Results show slight deviations from commissioning values due to MLC wear, highlighting the need for regular QA to maintain treatment accuracy and optimize machine-specific TPS calibration in radiotherapy.

T16 - JUNG Aleksandra Danuta

Readout conditions of lithium fluorite detectors after ultrahigh dose rate irradiation

T17 - KOZULJEVIC Ana Marija

Positron emission tomography imaging using quantum correlations of annihilation gamma-ray photons with single-layer Compton polarimeters

T18 - KUESS Peter

Investigation of Biases in AI-based Models for Radiation Oncology

T19 - LESO Aurora

the ISOLPHARM project

T20 - LIUZZO Mario Alexander

Optimizing Kidney Dosimetry Workflow in 177Lu-DOTATATE Therapy Through Single Time-Point SPECT/CT

T21 - MOHAMMADI Sara

Beam Quality Assessment: Evaluating Aluminum Purity's Effects

T22 - MOU Liliana

The LARAMED project at the INFN-LNL: Direct cyclotron-based production of medical radionuclides

T23 - MOURA BETTIO Tiago

In Vivo Dosimetry with GDCA in Particle Therapy: Variations in Secondary Photon Radiation Across Ion Species.

T24 - MOZZI Carlotta

Development and validation of a robust dataset using commercial TPS, radiochromic film and 2D diode matrix for deep learning in transit dosimetry

T25 - NAĐ Laura

Monte Carlo simulation of particle transport emitted during 123I decay: application in single-photon emission computed tomography

T26 - OBWEGS Christian

Evaluation of HyperSight Cone-Beam CT for Adaptive Radiotherapy: A Comparison with Conventional CT and Previous Detector Generations

T27 - PADOVANI Renato

Update of Italian diagnostic reference levels in interventional radiology

T28 - PADOVANI Renato

Update of Italian diagnostic reference levels in interventional radiology

T29 - PALENCIANO CASTRO Lidia

Monte Carlo analysis of dose deposition by alpha emitters in Targeted Radionuclide Therapy

T30 - PETERLIN Primoz

Metal implants, gas pockets, and intra-venous contrast – should automatic CT-ED conversion be trusted?

T31 - PETROVIC Veljko

Intercomparison of calibration factor of ionizing chambers in clinical practise

T32 - PÓCZA Tamás

Impact of knowledge-based treatment planning on adaptive radiotherapy for prostate cancer

T33 - POPOVIĆ Una

Comparative Dosimetric Analysis of Varian Halcyon and TrueBeam Platforms for Rectum and Inguinal Irradiation

T34 - PRIBANIĆ Ivan

Evaluation of Monte-Carlo-based Iterative SPECT Reconstruction: anthropomorphic phantom study

T35 - PWAMANG Caroline Kachana

Breast Density Patterns and Their Relationship with Breast Cancer among a Large Cohort of Ghanaian Women.

T36 - REGNER Michele-Louise

Evaluation of a New Multi-Energy QA Phantom for Spectral CT: Optimizing Diagnostic Imaging with Virtual Monochromatic Imaging and Metal Artifact Reduction

T37 - SAMAC Jelena Jovan

Radiation Exposure of Interventional Pain Physicians

T38 - SANTORO Benedetta

Monitoring of Indoor Air Quality to Prevent diffusion of Infection Diseases and improve Occupants' Safeguards

T39 - SARVARI Attila

Measurement of PDDs for the Xstrahl 200 orthovoltage therapy machine using the PTW Advanced Markus chamber

T40 - SAVATOVIC Sara

Acceptance testing and initial performance evaluation of the ARTIS Pheno C-arm system at Cattinara Hospital, Italy

T41 - SMILOVIĆ RADOJČIĆ Đeni

Impact of CT image data characterization on the absorbed dose calculation

T42 - STOJSIC Kristian

Automated VBQ determination from T1-weighted lumbar spine MRI data using a hybrid CNN-Transformer neural network

T43 - SUBIA POTOSI Maria Isabel

Geant4 based simulation of the GammaPod system

T44 - TOMSE Petra

SECURE project – Recommendations for minimization of radiation exposure in the isotope chain

T45 - VRBASKI Stevan

CT imaging through combined source- and detector-generated spectral separation

T46 - WESTERMAYER Moritz Johannes Martin

Evaluation of an almost-autonomous dosimetric workflow for the management of laryngeal cancer in radiotherapy

T47 - WOLF Lorenz

Collimated Carbon ion beams for preclinical in-vivo research

T48 - ZIMMERMANN Lukas

Evaluating the impact of DiffusionWeighted Imaging for Gross Tumor Volume delineation in cervical carcinoma patients

T49 - ZLATKOVA Ivona

Dosimetry and tracking accuracy evaluation of lung carcinoma treated with RADIXACT ^®TREATMENT DELIVERY SYSTEM and Synchrony Real-Time Delivery Adaptation using Dynamic Thorax Phantom 008A and CIRS motion platform.

T01

Comparison of DLG values obtained with five different measurement setups

Andrea Androcki [1] , Petra Seselja [2] , Nemanja Golubovac[1], Suzana Dovijarski-Stankin[1], Jelena Moravcevic[1], Milana Vezirovic [1,3], Borislava Petrovic[1,3]

[1]Oncology Institute Vojvodina, Sremska Kamenica, Serbia
[2]Faculty of technical Sciences, University Novi Sad, Novi Sad, Serbia
[3]Faculty of Sciences, University Novi Sad, Novi Sad, Serbia

Background

Determination of dosimetric leaf gap (DLG) and tongue and groove effect on MLC is a part of commissioning and validation procedure for a new linear accelerator and every available photon energy. It is a value that models the round-leaf-end effect of MLC and is of crucial importance for treatment planning calculation in radiotherapy.

Methods and materials

The methodology used for all measurements was sweeping gap technique by LoSasso, using files provided by Varian, later adapted for EPID. There were five different setups: ionization chamber in water in standard conditions, EPID, detector Octavius 4D manufactured by PTW, calculation in TPS in a water phantom generated in treatment planning system and compared to DLG values entered after commissioning and fine tuned by mock teatment plans and gamma analysis. This was done for three accelerators, and all available photon energies.

Results

Results are shown in Table 1. The TPS DLG values were obtained during commissioning by ion chamber measurements and were further optimized using mock clinical plans (prostate, head and neck and SRS brain plan), and evaluated by gamma analysis, and adopted as clinical values. All measured values were always smaller than fitted in TPS for clinical use, for all energies and all MLC types. The measurements by ionizing chamber and EPID were very similar, Octavius values were higher, and closer to optimized DLG values.

Table 1. Measured and calculated DLG values

Machine	Energy (MV)	DLG (mm)				
		0.6 cm^3 ion. chamber	EPID measured	Octavius measured	TPS calculated	In clinical use
Varian Edge 120 HD MLC	6FF	0,666	0,710	0,80	1,006	1,05
	6FFF	0,573	0,400	0,77	0,866	0,9
	10FF	0,761	0,865	0,94	0,426	1,4
	10FFF	0,713	0,581	0,82	1,129	1,1
Varian Vital Beam 120 Millenium MLC	6FF	1,582	1,541	1,88	1,777	1,8
	6FFF	1,653	1,234	1,69	1,658	1,7
	10FF	1,721	2,005	1,92	1,831	1,9
Varian True Beam 120 Millenium MLC	6FF	1,417	1,3	1,71	1,777	1,8
	6FFF	1,292	0,874	1,44	1,658	1,7
	10FF	1,580	1,506	1,62	1,831	1,9
	10FFF	1,480	1,281	1,50	2,113	2,1
	15FF	1,569	1,599	1,62	1,934	2,0

Conclusion and discussion

The measured DLG values by detectors differ from clinical TPS value, across all energies and MLC models, and are always smaller, probably due to the fact that the calculation equation in the manufacturer's method is based on the geometrical (nominal) relations of the gap size.

Literature

[1] LoSasso T, Chui C-S and Ling C C 1998, Physical and dosimetric aspects of a multileaf collimation system used in the dynamic mode for implementing intensity modulated radiotherapy Med. Phys. 25 1919–27

[2] Lin, CY., Shiau, AC., Ji, JH. *et al.* A simple method for determining dosimetric leaf gap with cross-field dose width for rounded leaf-end multileaf collimator systems. Radiat Oncol 13, 222 (2018). https://doi.org/10.1186/s13014-018-1164-1

[3] Ravindra Shendea, Ganesh Patel, Validation of Dosimetric Leaf Gap (DLG) prior to its implementation in Treatment Planning System (TPS): TrueBeamTM millennium 120 leaf MLC, reports of practical oncology and radiotherapy 22 (2017) 485–494, http://dx.doi.org/10.1016/j.rpor.2017.09.001

T02

Dosimetry from a Series of Whole-Body Planar Images and One SPECT/CT in Patients Undergoing Radionuclide Therapy using ^{177}Lu-labelled Radiopharmaceuticals

U. Beguš [1], P. Tomše[1], L. Jensterle [1], and L. Ležaič [1]

[1]University Medical Centre Ljubljana, Division of Nuclear Medicine

INTRODUCTION ^{177}Lu-labelled radiopharmaceuticals are increasingly used for therapeutic applications, particularly for the advanced gastroenteropancreatic neuroendocrine tumours (GEP-NETs) using somatostatin receptor-targeting ligands (^{177}Lu-DOTATATE) and a type of prostate cancer with PSMA-targeting ligands (^{177}Lu-PSMA). It's a standardized treatment, with a recommended dose of 7.4 GBq per cycle. However, response to therapy and uptake varies across patients, making dosimetry essential for evaluating absorbed doses to organs at risk (OARs). Various dosimetric software solutions are available for dose calculation. The objective of this work was to introduce the dosimetry protocol at the Division of Nuclear Medicine (DNM) in University Medical Centre Ljubljana (UMCL), and to compare the absorbed doses to OARs for patients treated with ^{177}Lu-labelled compounds.

MATERIALS/METHODS Post injection images were obtained from patients who were treated with ^{177}Lu-DOTATATE and ^{177}Lu-PSMA at the Division of Nuclear Medicine in UMCL. Whole-body planar images were acquired 0 h, 4 h, 24 h and 96 h after the administration of radiopharmaceutical, and one SPECT/CT was recorded after 24 h. Imaging was performed on a Siemens Symbia Intevo 2 SPECT/CT. Dosimetry was performed using OLINDA/EXM® software from HERMES. For ^{177}Lu-PSMA therapy, absorbed doses to the liver, kidneys and red bone marrow were evaluated, while for ^{177}Lu-DOTATATE, the kidneys, liver and salivary glands were considered limiting organs. Although the liver is not typically classified as an OAR in ^{177}Lu therapies, its dose should still be monitored.

RESULTS AND DISCUSSION Dosimetry was performed for 5 patients treated with ^{177}Lu-PSMA and 8 patients treated with ^{177}Lu-DOTATATE, who received an average activity of 7.5 GBq and 7.1 GBq, respectively. The absorbed doses to the kidneys were comparable between the two therapies (PSMA: 0.50 ± 0.17 Gy/GBq; DOTATATE: 0.70 ± 0.19 Gy/GBq). However, the liver dose was significantly lower in ^{177}Lu-PSMA patients (PSMA: 0.08 ± 0.07 Gy/GBq; DOTATATE: 0.86 ± 0.74 Gy/GBq), probably due to differences in liver tumour burden. The estimated absorbed doses to the bone marrow and salivary glands were 0.03 ± 0.01 Gy/GBq and 0.48 ± 0.37 Gy/GBq, respectively.
The calculated absorbed doses are consistent with reported absorbed doses for the kidneys (0.4–1.0 Gy/GBq), bone marrow (2–150 mGy/GBq), and salivary glands (0.5–1.9 Gy/GBq) [1].

SUMMARY We performed organ dosimetry using OLINDA/EXM software in patients who benefited from ^{177}Lu therapies. The calculated absorbed doses demonstrated interpatient variability, which can be associated with different patient characteristics. On account of this, establishing a standardized dosimetry workflow in clinical practice is essential, as it represents a step toward personalized targeted radionuclide therapy.

[1] Sjögreen Gleisner, K., Chouin, N., Gabina, P.M. et al. EANM dosimetry committee recommendations for dosimetry of 177Lu-labelled somatostatin-receptor- and PSMA-targeting ligands. Eur J Nucl Med Mol Imaging **49**, 1778–1809 (2022).

T03

The need for standardization of geometrical feature computation for dose prevision models in radiotherapy

Farah Ben Hammouda [1,2], **Lotfi Ben Salem** [3], **Raja Almijbari** [4], **Marco Esposito** [2]

[1] *Trieste University, Physics department, Trieste, Italy*
[2] *Abdus Salam International Center for Theoretical physics, Medical Physics, Trieste, Italy*
[3] *Salah Azaiez Institute, Radiotherapy department, Tunis, Tunisia*
[4] *National Cancer Center, Radiotherapy department, Benghazi, Libya*

Introduction;
The Overlap Volume Histogram OVH is a geometric feature that quantifies spatial relationships between the target and organs at risk (OARs) of a radiotherapy plan. This feature correlates with OAR dose and has been used extensively for dose prediction models and plan quality evaluation. OVH computation requires isotropic target expansion, despite the CT voxels' anisotropic nature. Different Treatment Planning Systems (TPS) vendors adopted varied approaches to accommodate this challenge. This could lead to potential inconsistencies, particularly in the absence of standardized methodologies. This study aims to quantify differences in OVH computation across multiple TPS and software, and to evaluate the impact on dose-correlation models.

Methods;
Nine CT series with corresponding structure were imported into three different commercial TPS (TPS1, TPS2, and TPS3), a research software package 3D slicer V5.6.1 and a custom-built MATLAB 2024ba (Mathworks) code. The target was expanded incrementally and its intersection with the heart was measured. The resulting curves from all five approaches were compared by analyzing heart volume overlap thresholds from 10-50% (R10%-R50%). These metrics were then correlated with heart mean dose (Dmean), and parameters of the linear models were compared across all methods.

Results;
Figure 1. shows that the relative differences for the five methods is ranging between 10% to 33%, for R10%, across all patients, and this trend is consistent across all R values. **Figure2.** Illustrates the relative differences across all Rs, for the intercept, values are ranging between 8% to 12% and for the slope, the relative differences are ranging from 7% to 17%.

Conclusion;
In this work we highlighted the OVH computation dependency on the TPS and software used, and its impact on the correlation models. Therefore, there is a need to standardize this geometric feature computation for a robust dose prevision modeling in radiotherapy.

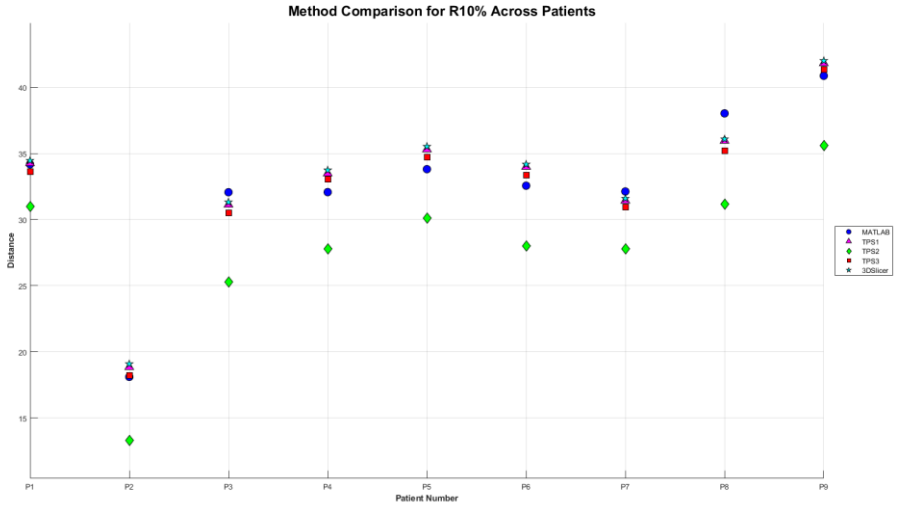

Figure 1.R10% computation across different patients using 5 different methods

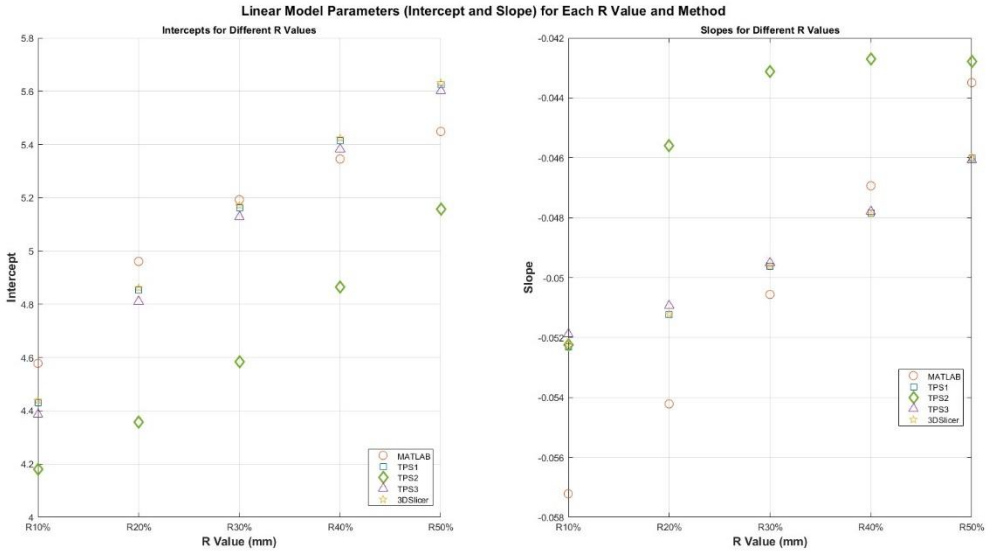

Figure 2.Linear model parameters of different Rs correlated with Dmean across the five methods; intercepts (left subplot), slopes (right subplot)

T04

Calculation of electron mass stopping power in the range 0.01−1000 MeV in different human tissues

Katarina Bito [1], Veljko Petrović [1], Jasmina Jeknić-Dugić [2]

[1] *University Clinical Center Niš, Niš, Serbia*
[2] *Department of Physics, Faculty of Sciences and Mathematics, University of Niš, Serbia*

Introduction

Knowledge of the nature of interaction of electrons with human tissue is of fundamental importance for the application in radiotherapy. The most clinically useful range of electron radiation is from 6 to 25 MeV. At these energies, electron beams can be used to treat superficial tumors (<5cm deep). In this paper, the mass stopping power of electrons from 0.01 to 1000 MeV was calculated for different human tissues using the programming language C. The obtained results were compared with the results of the ESTAR database [1].

Materials and Methods

For calculating the mass energy loss of electrons per unit path length through the human body, the following tissues and organs were selected: soft tissue, adipose tissue, bone, blood, skin, eye lens, lungs and brain. Collision losses were calculated using the Bethe-Bloch equation [2], both with and without considering the contribution of the polarization effect. The mass stopping power of electrons per unit path length due to radiation was calculated using the quantum electrodynamics formalism provided by Heitler [3]. The total mass stopping power of electrons is determined as the sum of the mass energy loss of electrons per unit path length due to collision and radiation, considering that the effects of each individual chemical element constituting the tissues and organs can be approximated by Bragg's rule [4].

Results and discussion

By analyzing the total mass stopping power and based on the obtained values for radiative and collision losses, it was observed that at energies up to 10 MeV, radiative effects contribute less than 10% to the total effect, with their influence gradually increasing with the rise in the kinetic energy of electrons, up to the critical energy. For therapeutic energy values, collision mass energy losses dominate. Skin is the organ most commonly treated with electron radiation, primarily at an energy of 6 MeV, where radiative effects account for 4.73% of the total.

References

[1] K. Bito, *Calculation of electron mass stopping power in the range 0.01-1000 MeV in different human tissues*, Master Thesis, Faculty of Sciences and Mathematics Niš, (2024)
[2] P. Mayles, A. Nahum, J.C. Rosenwald, *Handbook of radiotherapy physics, Theory and Practice*, Taylor&Francis Group, Boca Raton, Florida, (2007)
[3] P. E. Hodgson, E. Gadioli, E. Gadioli Erba, *Introductory Nuclear Physics*, Oxford University Press, (1997)
[4] F. H. Attix, *Introduction to radiological physics and radiation dosimetry*, WILEY-VCH Verlag GmbH & Co. KGaA, Weinheim, (2004)

T05

Evaluation of Patient-Specific Quality Assurance Software Mobius3D and VeriQA in Comparison to the Eclipse Treatment Planning System

Thomas Georg Boné [1] , **Peter Winkler** [1]

1 Universitätsklinik für Strahlentherapie-Radioonkologie, Medizinische Universität Graz

Patient-specific quality assurance (PSQA) plays a crucial role in ensuring the accuracy of dose calculations in radiotherapy. Independent secondary dose verification systems, such as Mobius3D and VeriQA, have been developed to independently validate treatment planning systems (TPS) like Eclipse. This study evaluates the performance of Mobius3D and VeriQA relative to Eclipse by analysing dose distributions, point dose agreements and other key clinical plan verification benchmarks.

A retrospective analysis was conducted on a cohort of clinical treatment plans using Eclipse (Varian Medical Systems), Mobius3D (Varian Medical Systems) and VeriQA (PTW). Dose calculations were compared using gamma index analysis, absolute dose differences and region-specific deviations. Additionally, the impact of heterogeneity corrections, field size variations and algorithmic differences on dose calculation accuracy was assessed.

Preliminary results indicate that while Mobius3D and VeriQA provide reliable secondary dose verification, discrepancies were observed in specific clinical scenarios, particularly in cases involving small fields and strong multi-leaf collimator (MLC) modulations. The influence of dosimetric leaf gap (DLG) correction factors, leaf modelling and tissue properties on dose calculation accuracy is also discussed.

Keywords: Radiotherapy, Treatment Planning System, Mobius3D, VeriQA, Eclipse, Dose Verification, Quality Assurance, Patient-Specific Quality Assurance.

T06

Workflow and Planning Techniques for Stereotactic Ion Beam Therapy in Treating Cardiac Arrhythmias

Ariadna Cherit Hernández [1,2,3], Claus-Stefan Schmitzer [2], Melanie Grehn [4], Oliver Blanck [4], Martina C. Fuß [2], Markus Stock[1,2]

[1]Karl Landsteiner Private University for Health Sciences, Krems, Austria; [2]MedAustron, Ion Beam Therapy Centre, Wr. Neustadt, Austria; [3]Medical University of Vienna, Vienna, Austria; [4]Department of Radiation Oncology, University Medical Centre Schleswig-Holstein, Kiel, Germany.

Ventricular tachycardia (VT) is the major cause for sudden cardiac death. Photon-based stereotactic arrhythmia radioablation (STAR) can significantly reduce VT burden in refractory patients [1]. On the other hand, proton beam radiotherapy (PBT) may offer better organ sparing for certain indications, due to its targeted energy deposition, but it is highly sensitive to motion, causing range uncertainties, and potential target under- or overdosing. Hence, advances in treatment planning, beam delivery, and motion management are crucial for precise treatment [2,3]. This study presents an end-to-end workflow for PBT STAR integrating electroanatomical mapping (EAM) data and analysing signal-triggering and beam-gating delays using the in-house Gating Interface Device (GID).

Three STAR PBT treatment plans, were generated and compared based on the STOPSTORM consensus nomenclature and constraints [4]. Dose evaluation indicated that all OAR constraints marked as high priority were met for Cases 1 and 2. For Case 3 the dose received by the pulmonary artery ($D_{0.03cc}$=25.14 Gy (RBE) slightly exceeded the clinical criteria ($D_{0.03cc}$<25.00 Gy (RBE)). Dose received by the stomach ($D_{0.05cc}$=13.73 Gy (RBE)) was close to the constraint ($D_{0.05cc}$<14.00 Gy (RBE)). PTV coverage at $D_{95\%}$ ranged from 23.33 Gy (RBE) to 24.46 Gy (RBE) while $D_{50\%}$ was 25 Gy (RBE) in all cases. For the TV (ITV overlap with left ventricle wall), no hotspots (D_{max}) greater than 33.60 Gy (RBE) were present. The TV $D_{95\%}$ ranged from 30.88 Gy (RBE) to 31.58 Gy (RBE). Overall, the treatment plans demonstrated effective OAR sparing, but target underdosing occurred due to sparing of the arteries and artefacts arising from ICD leads and left ventricle assist device (LVAD) in close proximity to the target. In all cases, the dose to the implantable cardioverter defibrillator (ICD) was 0.00 Gy fulfilling the constraint ($D_{0.1cc}$<2 Gy (RBE)), and the simulated times for beam allocation, delivery, and treatment room occupancy averaged 15.8, 19.6, and 40.9 minutes, respectively. The current standard treatment planning workflow takes 4–5 days—which might be too slow for critical VT patients (e.g., patients in electrical storm). Workflow enhancements envisioned include, extended DICOM worklists and testing setups for gated treatments using the GID, QA for EAM-to-CT target transfer, and ultrasound imaging for real-time beam synchronisation.

These findings lay the groundwork for integrating ion-based STAR into clinical practice. Future work will focus on end-to-end validation using an anthropomorphic phantom to assess motion-induced dosimetric changes and plan robustness through time-resolved dose measurements for different particles. Research will also explore motion control techniques and AI-driven auto-segmentation and auto-planning to streamline treatment for moving targets.

[1] M. Miszczyk, W. F. Hoeksema, K. Kuna, et al., Heart Rhythm 2024.
[2] B. Knäusl, L. P. Muren, Phys. Imaging Radiat. Oncol. **29** (2024).
[3] Y. Wang, H. M. Lu, Vis. Cancer Med. **5**, 4 (2024).
[4] V. Trojani, M. Grehn, A. Botti, et al., Int. J. Radiat. Oncol. Biol. Phys. **121**, 218 (2025).

Dosimetry analysis of different planning techniques of whole breast radiotherapy

T07

Suzana Dovijarski Stankin[1], Borislava Petrovic[1,2], Androcki Andrea[1], Nina Hajdin[1], Una Popović[1], Mirjana Papić[1]

1 Oncology Institute Vojvodina, Sremska Kamenica, Serbia
2 Faculty of Sciences, Department of Physics, University Novi Sad, Novi Sad, Serbia

Background: Radiotherapy of the breast is an integral part of breast cancer treatment, with maximum coverage of target and limitation of dose to organs at risk. Modern linacs offer different delivering techniques: three dimensional conformal techniques (3DCRT), intensity modulated radiotherapy (IMRT) and Volumetric Modulated Arc technique (VMAT) with the arcs mimicking tangential fields. The aim of this work is to compare and analyse advantages and disadvantages of these four techniques to targets and OARS.
Methods and materials: Ten right sided breast patients without nodal involvement were randomly selected for the purpose of the comparison. Four different plans were generated on the same set of structures, namely: 3DCRT plan, IMRT plan, and two VMAT plans: with partial continuous arcs and with arcs mimicking tangential gantry angles having avoidance sectors producing dosimetric "butterfly" effect. The plans were generated in treatment planning Eclipse v.15.6. Comparison of coverage, doses to OARs and low dose regions were analysed. The patients were treated with optimal treatment plan. Prescription was 40Gy in 15 fractions.
Result: Most important comparative data for OARs and target are given in table 1.

Table 1. Comparative data for target and OARS for four different planning techniques

Organs at risk (OARS)	Constraint	3DCRT	IMRT	VMAT butterfly	VMAT partial arc
Ipsilateral lung	**Dmean (Gy)**	7.44	6.56	7.67	7.85
Contralateral lung	**Dmean (Gy)**	0.22	0.19	0,47	1.4
	Dmax (Gy)	2.67	3.91	6.37	10.86
contralateral breast	**Dmax (Gy)**	5.72	8.64	10.3	13,0
heart	**Dmean (Gy)**	0.8	0.68	1.59	2.12
	Dmax (Gy)	6.92	8.67	10.93	9.92
Total time	**MU**	323	936	629	769

Target	**3DCRT**	**IMRT**	**VMAT butterfly**	**VMAT partial arc**
D98 (%)	88.59	93.9	94.46	95.42
D95(%)	98.13	98.8	99.13	99.26
Dmax (%)	106,5	106,9	109,5	109,3

Coverage and maximum doses have increased for advanced techniques as well as the homogeneity of delivery in comparison to 3DCRT. The volume of irradiated healthy tissue around the target was the largest for 3DCRT, the number of MU for IMRT. There was an increase in low dose volumes in inverse planning methods (V5Gy and V10Gy) of the ipsilateral lung, contralateral lung, and heart in comparison with 3DCRT, where only volume of lungs on the beam path was irradiated, with low dose region sharply cut at the beam edge. Mean lung dose is higher for advance techniques. Low dose volume of the contralateral breast and heart is higher for advanced techniques. Total MU is highest for IMRT (three fold than 3DCRT), which increases probability of backscatter in the body and gives additional unwanted dose to the tissues. There is no "best technique" as results depend on anatomy of the patient, but awareness on pros and contras of each technique is necessary. Surely, deep inpiration when available, is of great importance, but this set of patients did not include DIBH patients.
Discussion and conclusion: PTV coverage, conformity and homogeneity, in VMAT/IMRT are more superior than 3DCRT. Techniques with tangential field arrangement resulted generally in better OARs dosimetry compared to IMRT/VMAT. Low dose large volumes might have impact in secondary cancer induction in 10-15 years in patients younger than 40 years (at greater risk). Also liver toxicity should be taken into consideration due to increased number of modulated fields, greater scattering and dose leakage. Important task in future months would be to develop algorithm for decision making on technique to be applied in individual cases, and decide who exactly benefits from modulated techniques. Careful selection of patients should be our next step.

Literature:[1] Das Majumdar SK, Amritt A, Dhar SS, Barik S, Beura SS, Mishra T, Muduly DK, Dash A, Parida DK. A Dosimetric Study Comparing 3D-CRT vs. IMRT vs. VMAT in Left-Sided Breast Cancer Patients After Mastectomy at a Tertiary Care Centre in Eastern India. Cureus. 2022 Mar 28;14(3):e23568. doi: 10.7759/cureus.23568. PMID: 35494897; PMCID: PMC9045011.

T08

The Defect Perfusion Index: A New Descriptor for the Characterization of Myocardial Perfusion Imaging Systems

D. Dundara Debeljuh [1,2], R. Matheoud [3], O. Zoccarato[4], I. Pribanić [1,5], M. Brambilla [3], and S. Jurković [1,5]

[1] *Medical Physics and Radiation Protection Department, University Hospital Rijeka, Croatia,*

[2] *Radiology Department, General Hospital Pula, Pula, Croatia*

[3] *Medical Physics Department, University Hospital "Maggiore della Carità", Novara, Italy*

[4] *Unit of Nuclear Medicine and Department of Cardiology, S. Maugeri Foundation, IRCCS, Scientific Institute of Veruno, Veruno, NO, Italy*

[5] *Department of Medical Physics and Biophysics, Faculty of Medicine, University of Rijeka, Croatia*

Myocardial perfusion imaging (MPI) in nuclear medicine is performed to locate areas of the left myocardium ventricle where the blood flow may be reduced, i.e. areas of perfusion defects (PDs). The aim of this study was to evaluate the performance of various types of MPI systems in detecting PDs in simulated controlled and reproducible conditions. Descriptors for the characterization of MPI system (e.g. extent and severity of the PD, segmental uptake and global uniformity) have shown to be influenced by attenuation artifacts, partial volume effect, and quantitative post-processing algorithm used. Therefore, a new descriptor that minimizes abovementioned was introduced to further improve current MPI quality metrics [1].

Image data of anthropomorphic thorax phantom simulating normal and pathological myocardial perfusion conditions [2, 3] were acquired by different NaI-crystal detector systems with/without corrections for scatter and attenuation, and two CZT detector systems without corrections. Standard quantitative post-processing algorithms were used for polar map creation. Normal perfusion database for each MPI system was created by using phantom polar maps with normal myocardial perfusion conditions. Segmental values from normal databases and phantom polar maps with pathological perfusion conditions were used for the determination of the defect perfusion index (DPI). The DPI was used to evaluate the performance to detect small PDs in several positions inside simulated myocardium. Results showed that the D530c system outperforms other MPI systems in terms of PD detection, with the largest DPI values in all positions of interest. Results for DSPECT system revealed smaller mean DPI values compared to other MPI systems. Generally, it was shown that the PD position influences the DPI.

The DPI allowed one to investigate the intrinsic performance of the MPI system in detecting PD, minimizing the influence of attenuation artifacts and quantitative algorithm used. It can serve as an addendum to the metrics for the characterization of different MPI systems.

[1] D. Dundara Debeljuh, R. Matheoud, O. Zoccarato, et al. Characterization of myocardial perfusion imaging systems- an extension of quality metrics, Phys. Med. **125**, 104510 (2024).

[2] O. Zoccarato, C. Scabbio, E. De Ponti, et al. Comparative analysis of iterative reconstruction algorithms with resolution recovery for cardiac SPECT studies. A multi-center phantom study. J. Nucl. Cardiol. **21**(1) (2014).

[3] D. Dundara Debeljuh, R. Matheoud, I. Pribanić, et al. Evaluation of Single-Photon Emission Computed Tomography Myocardial Perfusion Detection Capability through Physical Descriptors. Appl. Sci. **14**(12), 5283 (2024).

T09

Towards optimized prescription metrics in novel radiotherapy techniques: A Machine Learning-guided study.

Alfredo Fernandez-Rodriguez [1,2], Yolanda Prezado[1,2,3,4]

[1](Presenting author underlined) Institut Curie, Université Paris-Saclay, Centre national de la recherche scientifique (CNRS) UMR3347, Inserm U1021, Orsay, France
[2] Université Paris-Saclay, Centre national de la recherche scientifique (CNRS) UMR3347, Inserm U1021, Signalisation radiobiologie et cancer, Orsay, France
[3] New Approaches in Radiotherapy Lab, Center for Research in Molecular Medicine and Chronic Diseases (CIMUS), Instituto de Investigación Sanitaria de Santiago de Compostela (IDIS), University of Santiago de Compostela, A Coruña, Spain
[4] Oportunius Program, Galician Agency of Innovation, Xunta de Galicia, A Coruña, Spain

Background
FLASH radiotherapy, microbeam radiotherapy (MRT) and minibeam radiotherapy (MBRT) are novel radiotherapy (RT) techniques that have been shown to improve healthy tissue sparing through unconventional dose delivery schemes, involving the usage of temporal, dosimetric and geometric parameters that differ from those in conventional RT. This study explores the influence of these parameters on the outcome of FLASH RT, MRT and MBRT irradiations using Machine Learning methods within current experimental evidence.

Methods
We analyzed six datasets of published preclinical MRT, MBRT and FLASH RT studies, training a Random Forest classification algorithm for predicting normal tissue toxicity, tumor control and increased lifespan (ILS) scorers of the irradiated groups. We quantified the influence of different key variables (e.g. peak, valley and average doses in MBRT and MRT, mean and pulse dose rate in FLASH RT or type of irradiated tissue) on the performance of our model over unseen data and ranked their importance on its predictive power.

Results
In MRT, valley dose was found as the most influencing physical parameters for healthy tissue sparing, while in MBRT the peak dose was highlighted as one of the most influential parameters, accounting for dose-volume effects that reduce healthy tissue tolerance at this greater field size. Valley dose showed a greater impact over ILS in a conjoint study of both techniques. In FLASH RT, the total dose, along with the tissue characteristics, were identified as the most influencing variables for tumor control and normal tissue toxicity with a reduced predictive power for the latter. The importance of dose rate was highlighted when considering therapeutic index.

Conclusions
Our results highlight how dose heterogeneity prevents healthy tissue damage in MBRT and MRT and the need of prescribing under critical tissue specific valley and peak dose values respectively for optimal sparing and tumor control. Our results also point at tumor control with FLASH RT being driven by the same mechanisms as in conventional RT, suggesting the need of a compromise with normal tissue sparing in the prescription of tissue-specific maximum doses.

T10

Ionoacoustic Dosimetry: Computational Simulations for Acoustic Detection of Proton and FLASH Electron Beams

Alessandro Michele Ferrara[1], Elia Arturo Vallicelli[2], Maurizio Marrale[3], Fabio Di Martino[5], Giuliana Milluzzo[4], Francesco Romano[4], Mattia Romeo[3], Mattia Tambaro[2], Marcello De Matteis[2]

[1]Department of Physics and Astronomy "Galileo Galilei", University of Padua, Italy
[2]Department of Physics, University of Milano-Bicocca, Milan, Italy
[3]Department of Physics and Chemistry, University of Palermo, Palermo, Italy
[4]Catania Division, National Institute for Nuclear Physics, Catania, Italy
[5]Centro Pisano ricerca e implementazione clinica Flash Radiotherapy Azienda Ospedaliero Universitaria Pisa AOUP, National Institute for Nuclear Physics Pisa Division, Pisa, Italy

Cancer remains a leading cause of mortality worldwide, with radiation therapy playing a crucial role in its treatment. Among advanced modalities, particle therapy offers the advantage of concentrating the radiation dose at the tumor site while minimizing exposure to healthy tissue, owing to its characteristic Bragg peak dose distribution. FLASH radiotherapy (FLASH-RT), an emerging approach that delivers ultra-high dose rates (UHDR), has shown promising therapeutic benefits by reducing normal tissue toxicity. However, dosimetry for UHDR, particularly in in-vivo settings, remains a significant challenge, limiting precise treatment planning and monitoring.

Ionoacoustic techniques have emerged as a novel method for radiation dose verification by leveraging the acoustic waves generated from energetic particle interactions. Under stress confinement conditions, the initial pressure distribution of these ionoacoustic waves is directly proportional to the absorbed dose. By simulating the acoustic propagation of the initial pressure distribution and applying a reconstruction algorithm, we present a promising approach for non-invasive, real-time dosimetry. In this study, we explore ionoacoustic dosimetry through computational simulations using the k-Wave toolbox in MATLAB to model acoustic signal propagation for 200 MeV proton beams and 9 MeV FLASH electron beams.

A large-scale 984×984 2D forward simulation in water was conducted using experimental data for the 9 MeV FLASH electron beam and a simulated 200 MeV proton beam. Interpolated Time-Reversal (ITR) algorithms were applied to reconstruct the initial pressure distribution based on sensor data. For 9 MeV FLASH electrons, γ-index analysis (1%/1 mm) showed that 82.33% of γ values were below 1.00 with 16 sensors, increasing to 97.86% with 32 sensors, 99.47% with 64 sensors, and 99.76% with 128 sensors. Similarly, for 200 MeV protons, 96.29% of values were below 1.00 with 64 sensors, reaching 99.66% with 128 sensors.

These results underscore the potential of ionoacoustic dosimetry for clinical applications. This approach could enable real-time, non-invasive dose verification, paving the way for improved efficiency, accuracy and monitoring in radiation therapy. Future research should focus on optimizing sensor design and refining reconstruction algorithms to facilitate clinical translation.

T11

Experiences with microcontroller supported DAP measurements

Csenge Forgács [1] , János Kiss [2] , Zsolt Dankó [2] and László Balkay [2]

[1] University of Debrecen, Faculty of Science and Technology, Institute of Physics
[2] University of Debrecen Clinical Centre, Department of Medical Imaging, Radiology

The University of Debrecen strives for accurate monitoring of patient doses from X-ray exposures in daily routine.

In connection with this, in collaboration with the International Atomic Energy Agency, a PTW-Freiburg Diamentor RS-KDK RS485 [1] type DAP measurement device has been acquired to measure the radiation emitted by X-ray planar imaging. This device is intended as a built-in solution, but the system has potential for development and automatization.

In this work, we created an autonom, portable measurement system with a 10000 mAh PD-capable power bank as a power supply. With the power bank-based supply during a continuous 1.5-hour measurement period, the charge dropped only from 100% to 77%.

Furthermore an RS485 communication between the Diamentor chamber and an external Arduino Nano [2] microelectronic device was also implemented and was found to be feasible. Via this method, calibration and correction coefficients and adjustment parameters could be effectively read out, as well as the measured DAP values which were sent to a PC.

With the built system we performed measurements on four nearly identical GE OPTIMA XR646 X-ray machines in order to compare their calculated dose-area products to our measured ones. These measurements took place at the Radiology Clinic of the University of Debrecen. We used 40 pairs of kV-mAs adjustment parameters to do the measurements.

As a result in both the calculated and measured mAs-DAP and kV-DAP relations, we could see the linear and polynomial increments on the depicted graphs which were expected from the literature [3,4]. In all cases, higher values were obtained from the X-ray machine's own calculations than the measured DAP data. This is beneficial for patient safety, given that it overestimates the true dose, but it could also be that the manufacturer is not using a DAP meter to validate the calculation. However, the discrepancy may also be due to the aging of the X-ray tube or a slight change in some other parameter.

In the future, comparing measured and calculated data may even lead to correction of DAP values in the DICOM metadata of images stored in the PACS system.

[1] DIAMENTOR RS-KDK Version RS232 (T11062) and Version RS485 (T11064) User Manual ver. 975.131.00/05 en

[2] H. K. Kondaveeti, N. K. Kumaravelu, S. D. Vanambathina, S. E. Mathe, S. Vappangi, A systematic literature review on prototyping with Arduino: Applications, challenges, advantages, and limitations, Computer Science Review, Volume 40, (2021)

[3] D.R. Dance S. Christofides A.D.A. Maidment I.D. McLean K.H. Ng, Diagnostic Radiology Physics A Handbook for Teachers and Students, International Atomic Energy Agency, Vienna (2014)

[4] P. Allisy-Roberts, J. Williams, Chapter 1 - Radiation physics, Farr's Physics for Medical Imaging (Second Edition), W.B. Saunders, 1-21, (2008),

T12

Optimization of a quantitative SPECT/CT reconstruction protocol: phantom measurements and preliminary clinical evaluation.

M.R. Fornasier [1] , F.A. Mayima [2], F. Dore[3], S. Prisco[3]

[1] Medical Physics Department, ASUGI (University Hospital), Trieste, Italy

[2] Advanced Master on Medical Physics, ICTP (Internationa Center for Theorethical Physics), Trieste, Italy

[3] Nuclear Medicine Department, ASUGI (University Hospital), Trieste, Italy

Introduction: Quantitative SPECT/CT analyzes medical images to extract numerical data in order to evaluate biological processes and tissues characteristics, both in diagnosis and therapy. Iterative quantitative reconstruction algorithms are currently available; they model physical characteristics of the acquisition process and incorporate the necessary corrections for quantitative SPECT, such as collimator-detector response, photon scatter, photon attenuation, partial volume artefacts. The accuracy of the quantitative software xSPECT was evaluated and the optimization of its configuration was performed by phantom measurements. The obtained results and some considerations about their use in clinical activity for the diagnosis of cardiac amyloidosis are presented.

Materials and methods: For the acquisitions, NEMA IEC phantom was used; the spheres and the background compartment were filled with homogeneous solutions of ^{99m}Tc-pertechnetate having concentrations of 35.1 kBq/ml and 5.8 kBq/ml, respectively. The xSPECT software was used to acquire and reconstruct the images. The optimization of reconstruction parameters, such as number of iterations, subsets and extent of the smoothing filter was based on measuring their impact on some quantitative metrics, such as Standardized Uptake Value, recovery coefficients, relative deviation, hot spot contrast, spatial resolution and coefficient of variation. Finally, some preliminary evaluations on reconstructed clinical images were carried out.

Results: For hot spheres, the parameter "maximum activity concentration" provides more accurate estimation of the real activity concentration than "peak" or "average" values, that underestimate it. The deviation of the measured values from the real values increases while the diameter of the spheres decreases, as effect of the spill-out. Moreover, the maximum activity concentration for the spheres of smaller diameters is closer to the real value in less smoothed reconstructions (10 mm filter); for the spheres of largest diameters, the evaluated concentration is closer to the real value when applying 13 mm filter; the application of 16 mm smoothing gives the worst results. Furthermore, increasing the iterations does not improve accuracy, while introducing much noise. Recovery coefficients and hotspot contrast reveal size-dependent effects of partial-volume correction. The best parameter to evaluate the background activity is the "average concentration", and it is not affected by reconstruction parameters. The overall results suggest that the best reconstruction has 24 iterations, 1subset and 13 mm Gaussian filter. However, in the preliminary evaluation of few clinical cases, the optimal setting seems to be 20 iterations, 1 subset, 10 mm filter, because it balances noise and details smoothing: increasing the iterations leads to very noisy images and increasing the Gaussian filter smooths to much the volumes with high uptake.

Discussion and Conclusion: The performance of the quantitative algorithm xSpect was evaluated and the best reconstruction parameters were established using a phantom study. However, application to clinical images required different settings; the need of further analysis of patients' images and adjustments to acquisition protocols in terms of acquisition time and administrated activity seems to be essential for accurate quantitative assessments in clinical practice.

T13

Estimation of fetal dose during head and neck radiotherapy: Comparing IMRT and VMAT techniques for iX and Halcyon radiation units

Elena Golaboska [1], Dushko Lukarski [2,3], Lambe Barandovski [4]

[1] City General Hospital 8th September, Skopje, Macedonia, [2] University Clinic for Radiotherapy and Oncology, Skopje, Macedonia, [3] Faculty of Medicine, Ss. Cyril and Methodius University, Skopje, Macedonia, [4] Institute of Physics, Faculty of Natural Science and Mathematics, Ss. Cyril and Methodius University, Skopje, Macedonia

Although cancer in pregnant patients is rare, it is not entirely excluded, and when radiation therapy is necessary, fetal safety remains a primary concern. This study investigates fetal radiation exposure in a multi-split composite phantom representing a five-month pregnant patient undergoing head and neck radiation therapy. The phantom was assembled from Sun Nuclear's Steev and Imrt thorax phantoms, extended with RW3 slabs simulating a pregnant abdomen. Dose measurements were made to assess fetal radiation exposure using a Farmer chamber at various points in the RW3 phantom which represent different locations of the fetus. We compared radiation doses from two types of linear accelerators and treatment techniques. One was a Varian iX linac, where we evaluated a typical static gantry intensity-modulated radiation therapy (IMRT), 7 coplanar beam treatment plan against a typical 3 arc volumetric modulated arc therapy (VMAT) plan. The second was a Varian Halcyon unit where we irradiated a typical 3 arc VMAT plan and compared it to the corresponding plan on the iX linac. A 6 MV beams were used for the iX linac, while a 6 MV FFF beams were used for the Halcyon unit. The treatment was envisioned as a standard treatment for the larynx in which 70 Gy are given in 35 fractions with 2 Gy/fr. Results showed that using VMAT the fetal dose was reduced by 39-53% (median 45%) at corresponding points compared to IMRT on the iX linac, demonstrating the advantages of arc-based techniques in minimizing unwanted exposure to the fetus. Additionally, treatment on the Halcyon reduced the measured dose by 21–37% (median 29%) compared to iX linac, likely due to the different MLC design, improved dose modulation and beam delivery efficiency. These findings highlight the importance of treatment technique and treatment unit selection in optimizing radiation therapy for pregnant patients. Based on these findings, we conclude that pregnant patients requiring radiation therapy should be treated with the Halcyon machine, as it provides superior fetal dose sparing while maintaining treatment effectiveness.

Keywords: head and neck cancer, fetal dose, iX linac, Halcyon, IMRT, VMAT.

[1] Yun Ming Wong, Calvin Wei Yang Koh, Kah Seng Lew, Clifford Ghee Ann Chua, Wenlong Nei, Hong Qi Tan, James Cheow Lei Lee, Michael Mazonakis, John Damilakis. A review on fetal dose in Radiotherapy: A historical to contemporary perspective. Physica Medica 105, 102513 (2023)

[2] Patrizia Kunert, Helmut Schlattl, Sebastian Trinkl, Edilaine Honorio da Silva, Detlef Reichert, Augusto Giussani . 3D printing of realistic body phantoms: Comparison of measured and simulated organ doses on the example of a CT scan on a pregnant woman. Medical Physics 51, 12 (2024)

T14

Challenges in introducing LUTATHERA® to clinical practice

L. Jensterle [1] , U. Beguš[1] , A. Sočan[1] , L. Ležaič[1] and K. Tomšič [1]

[1]University Medical Centre Ljubljana, Division of Nuclear Medicine

Introduction At Division of Nuclear Medicine in University Medical Centre Ljubljana radionuclide therapy with in-house produced Lu-177 labelled DOTATATE has been used for over 15 years to treat patients with neuroendocrine tumors. Dispensing system Tema Synergy Karl100 has been used for administration. Due to legal requirements we partly replaced in-house production with commercial radiopharmaceutical LUTATHERA® in 2024, which brought many technical challenges and radiation protection considerations that we needed to overcome. LUTATHERA® contains isotope Lu-177 with activity 7400 MBq and a long-lived component Lu-177m (half-life 260 days) which presents an important radiation protection consideration in case of contamination event. Due to large volume of 25 mL it was not possible to administrate LUTATHERA® with existing dispensing system. We decided to develop our own injection system following LUTATHERA® manufacturer's guidelines [1]. Before using system in vivo, we made several "cold" attempts without patient involvement to prove this method was safe and effective.

Materials and methods At first attempt, we developed a gravity method with an infusion pump, where peristaltic pump AGILIA (Fresenius Kabi) was flushing saline through short needle to vial with LUTATHERA® and consequently flushing it slowly through a longer needle to the patient. Activity in vial before administration and the residual activity was measured in activity meter. Due to LUTATHERA® vial being nearly full at 25 mL we faced problems of potential content spill over, large contamination and the possibility that not enough activity to be administrated to the patient. To avoid radioactivity spill over low flow rate of saline was needed which results in almost one hour duration of administration. We used lead radiation protection for the vial, lead glass window and added visual inspection with video camera to monitor spill over possibility.
To overcome occurring issues we received a special tubing system that allows the drug to be pumped from the vial by suction, followed by several flushes of saline to the vial to rinse all remaining radioactivity.

Results Functioning of the first method was proven to be satisfactory. Although with this method we were facing several content spill overs when the fluid level of the solution rose. Also, the content leftover activity in vial varied much between respective administrations from 1% to 10% of radioactivity content in vial and tubing.
Function of second method was proven much more effective and safer. There is minimum risk of spill over because the content is sucked out of vial. Furthermore, administration of the radiopharmaceutical to the patient was significantly shortened to half an hour. Also, the radioactivity leftover was always measured below 1%, likely due to several vial flushes with saline.

Summary We developed an effective semi-automatic administration method of LUTATHERA® that has low possibility of radioactivity contamination and is considerably safe from radiation protection standpoint. It administrates radioactivity to the patients with minimum activity leftover in the vial and the tubing system (together less than 1%). Although we will still examine the possibilities of improving and optimizing this method in terms of performance and radiation protection.

[1] https://www.ema.europa.eu/en/documents/product-information/lutathera-epar-product-information_en.pdf

T15

Multiple Energy MLC DLG verification and TPS data comparison, a study on Varian Clinac iX and Varian TrueBeam with Millenium MLC 120

phys. Nándor-Attila Juhász-Kollár [1] , phys. László Kóródi [1], Ágnes Wéber MD.PhD. [1]

Judit Olajos MD.PhD. [1]

[1]*Jósa András County Hospital, Nyíregyháza, Hungary*

Introduction

Accurate dose delivery in radiotherapy is critically dependent on the precise modeling of multileaf collimator (MLC) parameters, especially dosimetric leaf gap (DLG) and transmission factors. These parameters directly influence dose calculations, particularly in intensity-modulated radiotherapy (IMRT) and volumetric-modulated arc therapy (VMAT). Over time, MLC systems experience mechanical wear and calibration drift, which can lead to discrepancies in dose delivery.

This study aims to verify MLC DLG and transmission values for Varian Clinac iX and Varian TrueBeam linear accelerators, comparing them with their commissioning values. The measurements were carried out at the Department of Radiation Therapy, Jósa András County Hospital, Nyíregyháza, Hungary, using established Varian MLC QA protocols.

Materials & Methods

Measurements were conducted using a PTW Farmer ionization chamber, PTW Unidose E electrometer, and a 20×20 cm² water phantom at a 100 cm source-to-surface distance (SSD). The primary fields used were: Open fields for detector alignment and warm-up; Transmission fields to measure leakage through MLC leaves; Sliding gap fields at various gap sizes (2–20 mm) to assess the MLC's mechanical behavior and dose leakage.[1] These measurements were performed for multiple photon energies: 6 MV, 10 MV, 15 MV, and 16 MV.

Results & Discussion

The results revealed that the DLG and transmission factors for both linacs increased slightly from their commissioning values. For the Clinac iX, the DLG values were slightly higher than the commissioning values, likely due to wear and tear in the MLC system over time. Similarly, the TrueBeam also exhibited a slight increase in DLG, but transmission factors were generally lower than those of the Clinac iX, suggesting that the TrueBeam's MLC system has better leaf sealing and lower leakage. These findings underscore the importance of regular MLC quality assurance (QA) to detect small variations that could potentially impact dose accuracy. Even small changes in DLG can affect the precision of dose calculations in complex treatment plans. Additionally, the slight differences in transmission between the two machines highlight the need for machine-specific QA protocols.

Conclusion

This study confirms the importance of routine MLC QA to ensure accurate dose delivery in radiotherapy. Although the variations observed were small, they illustrate the potential for changes in MLC performance over time. Regular MLC verification is necessary to maintain the accuracy of treatment planning systems (TPS), ensuring that patients receive the prescribed dose with minimal deviations.

Routine MLC QA is crucial for maintaining the accuracy of treatment planning and dose delivery.

Slight deviations in DLG and transmission can affect clinical outcomes, highlighting the need for recalibration and adjustments.

Differences between linacs show that machine-specific QA procedures are essential for reliable and accurate treatment.

[1] Official Varian Teaching Course material – Dosimetric Leaf Gap Measurement (2010)

T16

Readout conditions of lithium fluorite detectors after ultrahigh dose rate irradiation

Aleksandra Jung [1] , Agata Czuk [1] , and Jan Swakon [2]

[1] AGH University of Krakow, Faculty of Physics and Applied Computer Sciences, Krakow Poland

[2] Institute of Nuclear Physics Polish Academy of Sciences, Krakow, Poland

FLASH radiotherapy is a novel technique that uses ultrahigh dose rates (UHDR) to potentially spare normal tissue without sacrificing tumour control. UHDR dosimetry and beam monitoring are challenging; therefore, both active (e.g. calorimeters and ionisation chambers) and passive dosimeters (thermoluminescence and optically stimulated dosimeters) are under investigation. It is also important to understand the effects that will influence the detector response and to minimise the uncertainty of the measurement protocol. Detailed studies dedicated to the analysis of thermoluminescent detectors readout protocol are scarce [1-3]. For that reason, the goal of the study was to verify the influence of different filters applied for thermoluminescence signal readout of lithium fluoride detectors irradiated ultrahigh doses to recommend filters optimal for high precision signal measurements.

In this study, LiF: Mg, Cu, P and LiF: Mg, Ti detectors, commercially known as MCP-N and MTS-N, respectively (produced at the INP, Krakow, Poland), were applied. A proton beam from the AIC-144 cyclotron 60 MeV at Krakow Institute of Nuclear Physics Polish Academy of Sciences with a high dose rate at the level of 50 Gy/s was used twice for detector irradiations. Doses were in the range of 12-100 Gy. The thermoluminescence signal was measured in standard mode, except filtration conditions, including pre-exposure annealing at 240°C/10 minutes for MCP-N, 400°C/2 hours, and 100°C/1 hour for MTS-N; exposure; post-exposure annealing at 100°C/10 minutes; and readout at 2°C/s to 245°C and 280°C for MCP-N and MTS-N, respectively (TL/OSL *lexygresearch* reader). Two typically available sets of filters were applied: wide–band blue filter (set 1: a combination of filters SCHOTT BG39, SCHOTT BG25, SCHOTT KG 3 plus grey filter 0.01%) and so-called filter TL > 530 nm (set 2: OG530, SCHOTT KG 3). The area under the peak and the amplitude were utilised for dose estimation, linearity, and reproducibility analysis.

Since the doses are much higher than in standard radiotherapy, the number of counts is also higher, and often too high for a photomultiplier readout. Additional filtration of the measured signal must be applied. The shape of thermoluminescence curves was more repeatable for set 1 of filters than for set 2 of filters. Results showed linear dose dependence, but adequacy was different for different filters. As MTS-N detectors have a twice lower sensitivity for low doses (up to 20 Gy) additional filtration is not required in that range.

Lithium fluoride detectors may be employed for ultrahigh dose rate proton beam measurements when filter set 1 is applied, according to preliminary results. Further studies related to the stability and repeatability of the signal are continued.

[1] A. Subiel, F. Romano. Br. J. Radiol. **96**, 20220560 (2023).

[2] F. Romano et al. Med Phys. **49**, 4912 (2022).

[3] S. Motta et al. Physics in Medicine and Biology, **68**, 145007 (2023).

T17

Positron emission tomography imaging using quantum correlations of annihilation gamma-ray photons with single-layer Compton polarimeters

A.M. Kožuljević[1,2], Tomislav Bokulić[1], Darko Grošev[3], Zdenka Kuncic[4], Siddharth Parashari[1], Luka Pavelić[2], Petar Žugec[1], Marijan Žuvić[3] and Mihael Makek[1]

[1]University of Zagreb Faculty of Science, Bijenicka Rd. 32, Zagreb
[2]Institute for medical research and occupational health, Ksaverska Rd. 2, Zagreb
[3]University Hospital Centre Zagreb, Kispaticeva street 12, Zagreb
[4]The University of Sydney, School of Physics, Camperdown, NSW 2050, Australia

Positron emission tomography (PET) is a very successful medical imaging modality, utilizing positrons' annihilation with electrons in a patient's tissue, but still suffers from drawbacks such as relatively long acquisition times and low signal-to-noise ratio (SNR) due to scatter and random coincidences [1]. One of the possible improvements to PET imaging could come from measurements of quantum correlations of annihilation gamma-ray photons, which are entangled in their polarizations. This property is not yet utilized in conventional PET scanners that use only their 511 keV energy and opposing momenta for coincidence identification. The initial orthogonality of their polarizations is evident in the difference in their azimuthal Compton scattering angles, which can be measured with single-layer Compton polarimeters [2]. The advantages that these measurements offer are possible SNR and signal-to-background ratio (SBR) enhancements in images since the random coincidences lack this property [3, 4, 5]. To explore this possibility, we built a PET demonstrator, consisting of four detector modules mounted on a circular construction capable of rotation, emulating the full ring of detectors. The modules are segmented scintillating detectors coupled to silicon photomultipliers, assembled from 16x16 crystals (GAGG(Ce) and LYSO(Ce)) with a matrix pitch of either 3.2 mm or 2.2 mm. The device was tested at the University Hospital Centre Zagreb with sources that have clinically relevant activities: two line Ge-68 sources (1.6 mm in diameter, activity ~45.5 MBq) and NEMA phantom filled with Ga-68 (NU 4-2008, initial activity ~400 MBq). OMEGA software for image reconstruction was utilized in MATLAB environment, and images were created with the *Ordered Subset Expectation Maximization* (0SEM) reconstruction algorithm. We will show the images obtained from the two Ge-68 sources, as well as the NEMA phantom filled with Ga-68, reconstructed solely from polarization-correlated annihilation quanta, and compare them to ones obtained conventionally from photoelectric interactions [6]. The measurements of the polarization-correlated gamma-ray photons also show up to 40% increase in signal-to-random-background compared to measurements of the photons with single-pixel interaction, however keeping the equivalent spatial resolution remains challenging. We will discuss the possible improvements in PET demonstrator device and signal-to-background enhancements by measuring the polarization correlations of the annihilation quanta.

[1] S.R. Cherry *et al*., J Nucl Med. **59**(1), 3-12 (2018).
[2] M. Makek *et al*., Nucl. Instrum. Methods Phys. Res. A **958,** 162835 (2020).
[3] Z. Kuncic *et al.,* Nucl. Instrum. Methods Phys. Res. A, **648**, S208–S210 (2011).
[4] D.P. Watts *et al.,* Nat. Commun., **12**, 2646 (2021).
[5] D. Kim *et al.,* J. Instrum. **18**(07), P07007 (2023).
[6] A. M. Kožuljević *et al*., Nucl. Instrum. Methods Phys. Res. A, **1068**, 169795 (2024).

T18

Investigation of Biases in AI-based Models for Radiation Oncology

Peter Kuess[1] , Gerd Heilemann[1] , Dietmar Georg[1], Borislava Petrovic[2]

[1] Department of Radiation Oncology, Medical University Vienna, Austria
[2] University of Novi Sad, Oncology Institute of Vojvodina, Serbia

Automation based on AI-based models holds great promise in advancing Radiation Oncology covering fields like structure segmentation, quality assurance, and treatment planning. However, such models may be affected by biases, stemming from differences between training data and customer data. Those differences can lead to inferior results of the model and in worst case to a deteriorated treatment.

This study aims to identify and quantify such biases in AI-based models, focusing on automated treatment planning, by comparing data from two institutions (Institute A and B). Variations in treatment workflows, imaging protocols, contouring practices, time-to-treatment intervals, institutional protocols, quality assurance procedures, and more may introduce discrepancies.

70 low- and medium-risk prostate cancer patients (51 from institute A and 19 from institute B) were evaluated in a retrospective analysis. To capture geometric representations of each patient, a set of 12 anatomical features was calculated for the prostate, bladder, and rectum, including, Euclidean distances between structure centroids, overlap measures (DICE coefficient), and shape features (surface area, elongation).

A principal component analysis (PCA) was performed to identify the main factors contributing to potential biases. To reduce complexity and noise due to colinear features, correlation between features were calculated. From any pair with correlation of less than 0.6 only one features was kept as input for the PCA. Both institutions used a SOMATOM Definition CT scanner (Siemens Healthineers, Germany) with a pixel size of 0.977×0.977 mm and a 2 mm slice thickness. Organ at risk delineation at Institute A was performed using an AI-based algorithm (Therapanacea, France), while delineation was a manual process at institute B. Only institute A used a rectal balloon for all prostate cancer patients. Differences in the applied bladder filling protocols were observed.

The PCA suggested that the two patient cohorts have distinct characteristics captured by the first two principal components (PC) (see Fig. 1). The separation of the two cohorts was more prominent along PC2, indicating that the key features contributing to PC2 were likely driving the differentiation between the cohorts. In detail these features included, prostate-bladder, prostate-rectum, and rectum-bladder overlap, as well as shape metrics (e.g. elongation and surface area).

This study highlights the importance of understanding and addressing biases in AI-based models for radiation oncology. Only some differences between the features of both cohorts could be explained by the use of a rectal balloon in institute A (e.g. prostate-rectum distances). General differences in the structure shapes and spatial relationships between structures can influence any AI-based model in this context. Identifying and quantifying feature-level discrepancies between datasets can help generalize AI models that aim to improve radiation oncology workflows. In the next phase we will investigate if the same AI-based automation can reduce the variance along the principal components seen in the different cohorts.

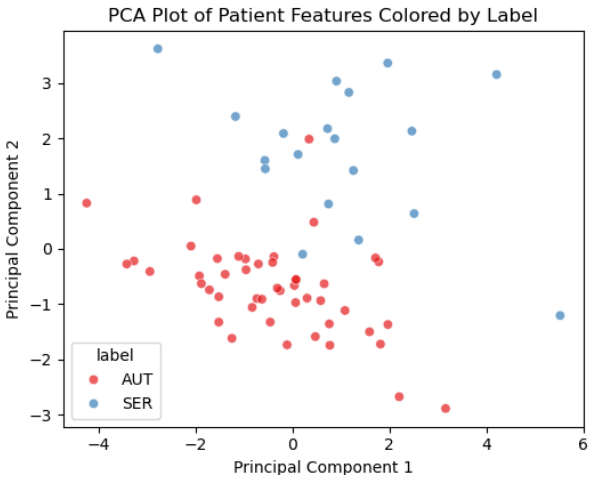

Figure 1: Distribution of cohort A and cohort B by two principal components. The separation between both cohorts is mainly along PC2.

T19

The ISOLPHARM collaboration

A. Leso [1]

Univeristà degli studi di Ferrara

INFN-LNL

ISOLPHARM is a multidisciplinary project aiming to study a new and unconventional method for the production of pure radionuclides based on the Isotope Separation On-Line (ISOL) technique and to develop a new generation of radiopharmaceuticals. As one of the applications of the SPES project (Selective Production of Exotic Species), ISOLPHARM will exploit the Radioactive Ion Beams (RIBs) produced at the ISOL SPES facility, currently under construction at the Legnaro National Laboratories (LNL) of INFN.

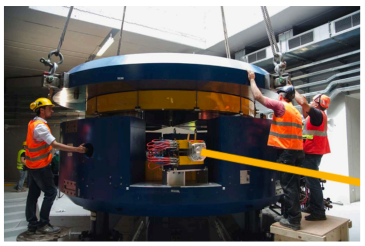

SPES Proton Driver (Cyclotron)

In the last few years, the project has been focusing on the beta-emitter silver-111 as a possible theranostic candidate for radiopharmaceutical therapy.
The latest experiment of this project, named **ADMIRAL**, focuses on the evaluation of the diagnostic and therapeutic power of radiopharmaceuticals containing the aforementioned radionuclide. This experiment is divided in 4 main work packages:

- **WP1, radiopharmaceutical production and in vivo testing**: optimize the radioisotopic production and purification of silver-111 via traditional methods since the ISOL technique is not available. Due to the ongoing SPES construction, the TRIGA Mark II nuclear reactor at L.E.N.A. is still involved for the production. Radiochemistry experiments are currently underway to dissolve irradiated targets and extract silver-111. Concurrently, researchers are developing methods to integrate these radionuclides into macromolecular structures that can effectively bind to and transport them to tumor tissues, with the goal of specifically targeting cancer cells. In this work package is located even the series of in vivo experiments conducted at Capir (CT). At the beginning of this year the first test with silver-111 has been conducted, studying the biodistribution of the free radionuclide at different times after the injection in mice. The shown image represents one of the mice one hour after injection and is obtained with Bruker Xtreme.

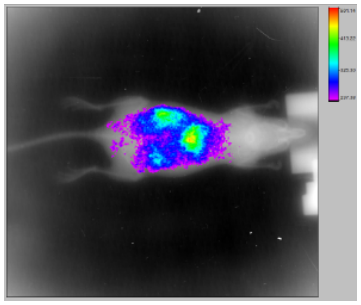

- **WP2, beta-imaging**: design, construct, and characterize a device that utilizes monolithic silicon pixel technology (ALPIDE chips) to capture high-resolution "β-pictures" of 2D cellular cultures or thin 3D slices (scaffolds) containing β-emitters.

- **WP3, gamma-imaging**: design and characterize a γ-camera for detecting γ radiation emitted during the decay of silver-111.

- **WP4, targeted radiobiology**: study the effects of silver-111 targeted radionuclide therapy on cell survival using a "targeted" radiobiology approach. In particular, the first survival experiments with free silver-111 have been conducted on UMR-106 cells in March 2024, planning to test the chelated and targeted silver-111 molecule by the end of the year.
  Concurrently, 3D scaffold production is being explored with the aim of developing a protocol for studying the effects of silver-111 in this specific geometry. Finally, the radiobiological data are

correlated with the absorbed dose at the cellular level, computed using the Monte Carlo method (Geant4, Geant4-DNA), and results are compared with other radionuclides used for therapy and diagnostics.

T20

Optimizing Kidney Dosimetry Workflow in 177Lu-DOTATATE Therapy Through Single Time-Point SPECT/CT

Abstract:

Background:

177Lu-DOTATATE therapy plays an increasingly important role in the treatment of advanced neuroendocrine tumors. Since the kidneys are considered the dose-limiting organs, renal dosimetry is essential. However, dosimetry procedures require dedicated software, human resources, and significant imaging workload, especially in multi-time-point protocols. This study aims to develop an optimized protocol to estimate kidney absorbed doses using a single SPECT/CT acquisition.

Materials and Methods:

Renal dosimetry was performed on 30 patients undergoing standard 177Lu-DOTATATE administration (4 cycles of 7.4 GBq). A tomographic sensitivity calibration for 177Lu was carried out using a Discovery 670 GE SPECT/CT system. The dosimetry workflow for each cycle included:

(1) single time-point SPECT/CT acquisition at 96 hours post-injection;

(2) kidney segmentation on CT images;

(3) dose calculation based on the SPECT data using the method proposed by Hänscheid.

Results:

The analysis demonstrated the feasibility of this simplified workflow. Cumulative renal doses in all patients remained below the threshold values of 23–28 Gy. ANOVA comparison between cycles showed no statistically significant differences ($p > 0.05$). The average total dose to the right kidney was 9.0±2.6 Gy and 8.7±2.7 Gy to the left kidney.

Conclusions:

This study presents an optimized workflow for renal dosimetry in 177Lu-DOTATATE therapy using a single SPECT/CT acquisition and open-source software tools. The approach may also be applied to other therapies such as 177Lu-PSMA and extended to dosimetric evaluations of other organs.

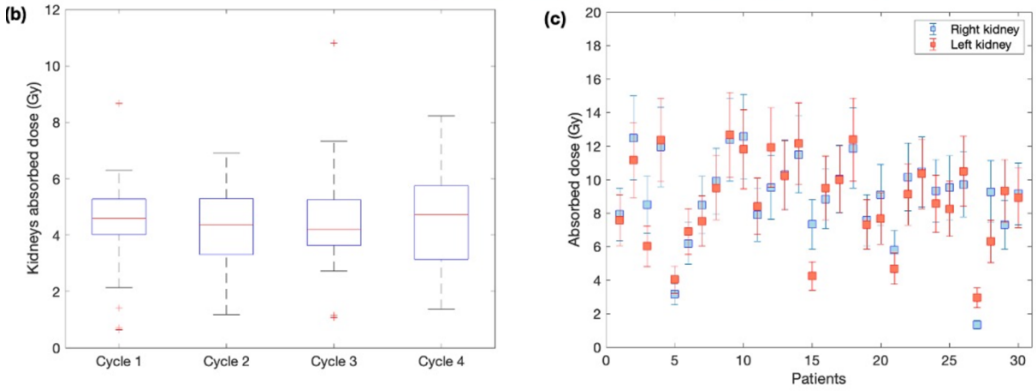

[1] Emami et al. Tolerance of normal tissue to therapeutic irradiation. Int J Radiat Oncol Biol Phys. 1991;21:109–22.

[2] Hänscheid et al. Dose Mapping After Endoradiotherapy with ^{177}Lu-DOTATATE/DOTATOC by a Single Measurement After 4 Days. J Nucl Med. 2018;59(1):75-81.

T21

Beam Quality Assessment: Evaluating Aluminum Purity's Effect

Sara Mohammadi[1], Joshua Deslongchamps[1], Jiali Wang[1], MaryEllen Jafari[1]

1) Kaiser Permanente Southern California, Los Angeles, CA

We aim to evaluate Aluminum purity's effects on Half Value Layer (HVL)measurements and beam quality across mobile and fixed radiographic units. Beam quality assessment is fundamental aspects of ensuring the safe and effective delivery of ionizing radiation. Standards for this assessment vary nationally and internationally leading to ambiguity within measurements which may cause regulatory issues.

Comparing FDA regulation and IEC standards, there is a discrepancy on purity of reference Aluminum used for determining HVL [1,2,3]. FDA requires Type-1100 aluminum (with a minimum of 99.0% purity), while IEC requires a minimum of 99.9% purity. We measure the effect of Al sheets of 99.0% and 99.5% purity, observing a noted difference in HVL values. Measurements were performed on mobile and fixed radiographic units utilizing detectors from three manufacturers. Methods and setup were built using IEC standards for HVL measurements with techniques chosen for the standard patient. Exposures were taken across a range of thicknesses of aluminum in small increments centered around the projected HVL. Through exponential fitting of exposure versus Al thickness, HVL was determined. Additionally, for each solid-state detector, a single-shot HVL measurement was performed without aluminum in the x-ray beam.

The results show HVL measurements increased by 1.35% to 4.82% with a median increase of 3.26% when going from 99.0% to 99.5% purity. Comparing the single-shot value to the interpolated values with 99.0% Al and 99.5% Al, 99.0% deviation ranged between 0.16%-8.99% with a median of 4.90% while 99.5% ranged between0.43%-4.79% with a median of 2.62%.

These deviations are significant and would be more substantial using 99.9%Aluminum. Such discrepancy can result in units falsely failing HVL assessments due to different types of aluminum used in manufacturing vs measurements. More stringent or clear guidelines should be defined for HVL measurement.

[1]: 21 CFR, part 1020 Code of Federal regulation, 1020.30

[2]: IEC 60522-1, Determination of quality equivalent filtration & permanent filtration

[3]: IEC 60522-2, Guidance on quality equivalent filtration & permanent filtration

T22

The LARAMED project at the INFN-LNL: Direct cyclotron-based production of medical radionuclides

Liliana Mou [1], Gaia Pupillo[1], Lucia De Dominicis[2], Sara Cisternino[1], Alisa Kotliarenko[1] and Juan Esposito[1]

[1]INFN, Laboratori Nazionali di Legnaro, Viale dell'Università 2, 35020 Legnaro (Padova), Italy

[2] Dipartimento di Fisica e Astronomia, Università di Padova, Via Marzolo 8, 35131 Padova, Italy

The cyclotron-based production of medical radionuclides is one of the research activities carried out in the framework of the SPES (Selective Production of Exotic Species) project at the Legnaro National Laboratories of the National Institute for Nuclear Physics (INFN-LNL). The heart of SPES is the 70 MeV proton-cyclotron with a dual-beam extraction that will enlarge the possibilities related not only to nuclear physics and astrophysics studies but also to applied research, including radionuclides production for medical applications [1]. The interdisciplinary LARAMED (LAboratory of RAdionuclides for MEDicine) project [2,3] is based on the direct-activation method to produce several innovative medical radionuclides. The LARAMED project's aim is to complete the entire production cycle, starting from the target manufacturing and nuclear cross section measurements to the radiopharmaceutical production. To achieve these goals the LARAMED facility is currently under completion and it includes:

- two different bunkers devoted to: (i) the production of limited amounts of novel radioisotopes for research purposes (i.e., support other research centers, as well as research studies at the preclinical level) by using high-current proton beam and (ii) experimental nuclear physics activities (i.e., mainly cross section measurements) by using a maximum current of 100 nA;
- two different laboratories respectively dedicated to target manufacturing and radiochemical separation and characterisation of the obtained product.

At SPES both the target station and the target-holder have been designed and realized specifically for the cross section measurements. Waiting for the completion of the two LARAMED bunkers, we had the opportunity to use a different bunker temporarily. The use of the target station was therefore successfully tested and, in the future, it will be used for cross section measurements for the production of radioisotopes of medical interest. This work will present the results of these preliminary tests and the experimental activities currently underway.

[1] G. Pupillo et al., Eur. Phys. J. Plus 138, 1095, (2023), doi: 10.1140/epjp/s13360-023-04564-3
[2] J. Esposito et al., Molecules 24(1), 20, (2019), doi: 10.3390/molecules24010020
[3] G. Pupillo et al., Journal of Radioanalytical and Nuclear Chemistry 333, 1487-1496, (2024), doi: 10.1007/s10967-023-09075-0

T23

In Vivo Dosimetry with GDCA in Particle Therapy: Variations in Secondary Photon Radiation Across Ion Species.

By Tiago Bettio

Heavy particle radiotherapy is a highly advanced form of cancer treatment that uses high-energy particles, such as protons, helium, or carbon ions, to target and destroy tumor cells with minimal damage to surrounding healthy tissues. Radiation dose measurements and calculations are critical aspects of this therapy. Due to the particles high Linear Energy Transfer (LET), accurate dosimetry is essential to ensure optimal treatment outcomes. When irradiated with heavy particles, Gadolinium emits a very specific photon energy spectrum showing promising potential for use *in vivo* dosimetry techniques.

The photon flux generated depends on the type of particle used in the beam, so analyzing the peak signal relative to the equivalent dose could be useful to determine whether spectroscopic techniques might be applied for *in vivo* dose measurement.

In this work Monte Carlo MCNP6 code was used to simulate experimental setup to investigate the code's capability to simulate this spectrum. The findings indicate that the MCNP6 cascade mode, employing the CEM03.03 model, yields accurate predictions for proton beam interactions. However, it significantly underestimates the photon flux, with discrepancies amounting to a factor of 3.2 for helium ions and 54.7 for carbon ions. The equivalent dose for these particles shows that carbon ions produce the strongest signal per ion per mSv.

Keywords: Radiotherapy, Dosimetry, Heavy Particles.

T24

Development and validation of a robust dataset using commercial TPS, radiochromic film and 2D diode matrix for deep learning in transit dosimetry

C. Mozzi [1,2], Marini L.[3,4], Avanzo M.[5], Lizzi F.[4], Marrazzo L.[1,6], Meattini I.[1,6], Pirrone G.[5], Retico A.[4], Kraan A.[4], Talamonti C. [1,2,5]

[1]Univesity of Florence – Italy, [2]INFN Florence -Italy, [3]Univesity of Pisa – Italy, [4] INFN Pisa - Italy, [5] Centro di Riferimento Oncologico (CRO) di Aviano -Italy, [6] Careggi University Hospital, Florence – Italy

This study aims to develop and validate a dataset for training a deep learning (DL) model for transit dosimetry using an electronic portal imaging device (EPID). The dataset comprises more than 200 EPID images and their corresponding portal dose (PD) distributions, calculated with the Monte Carlo dose calculation algorithm within the Monaco treatment planning system (TPS) at the EPID level. The first step involved validating the TPS by comparing its output to radiochromic film dosimetry and the 2D diode array MapCheck2.

Transit dosimetry was simulated by calculating the dose distribution at the EPID level, 60 cm from the isocenter. The EPID geometry was modeled with a 4.4 cm thickness and a relative electron density of 1. The resulting dose map was centered. Gafchromic (GAF) EBT3 films were placed at the EPID level to validate the simulations. The setup used a water-equivalent thickness in place of the EPID detector. Seven GAF films were analyzed, showing good agreement between measured and calculated dose distributions, with a gamma passing rate around 90% using the 5%/5 mm global criteria. However, the accuracy was influenced by scanner variability, film positioning, and post-irradiation scan timing. To improve the validation, MapCheck2 was also used at the EPID level. This provided better agreement, with a median local gamma passing rate of 98% using the 5%/5 mm criteria and 90% using the 3%/3 mm criteria. Various homogeneous multi-plug phantoms with inserts of titanium, bone, solid water, and lung tissue, as well as anthropomorphic phantoms, were irradiated using different beam geometries and dose levels. After confirming the TPS response accuracy, over 200 EPID images paired with simulated dose images were generated to create a robust dataset for DL model training.

The DL model, trained on this dataset, demonstrated high performance, achieving a 99% gamma passing rate using the 3%/3 mm criteria for dose distribution predictions from EPID grayscale images. This study shows that Monaco TPS can accurately calculate dose distributions at the portal image level across a variety of phantoms and that DL models can be successfully trained for EPID transit dosimetry in radiotherapy.

[1] Zhang J., A. et al., *Radiat. Oncol.* 17, 31 (2022).
[2] Marini L., B. et al., *Nucl. Instrum. Methods Phys. Res. A* 1069, 169908 (2024).
[3] Santos T., *Radiat. Phys. Chem.* 179, 109217 (2021).
[4] Marrazzo L., A. et al., *Phys. Med.* 31, 1035-1042 (2015).
[5] Song J. Y., et al. *Med. Dosimetry* 39, 134-138 (2014).

T25

Abstract for the poster

Monte Carlo simulation of particle transport emitted during ^{123}I decay: application in single-photon emission computed tomography

L Nađ [1], I Pribanić [1, 2]

[1]Medical Physics and Radiation Protection Department, University Hospital Rijeka, Croatia,
[2]Department for Medical Physics and Biophysics, Faculty of Medicine, University of Rijeka, Croatia

This study analyzes the influence of different collimators on the quality of image data when using ^{123}I in single-photon emission computed tomography (SPECT). While the low-energy high-resolution (LEHR) collimator is most often used for ^{123}I, it is not optimal for its energy spectrum [1, 2]. This study explores the potential of using low-penetration high-resolution (LPHR) and medium-energy (ME) collimators to enhance image data quality.
The SIMIND Monte Carlo simulation algorithm was used to perform nine simulations with a NaI(Tl) scintillation detector and three collimators (LEHR, LPHR and ME) [1]. Simulations included a point source, a cylindrical source and a Jaszczak phantom with rods and spheres simulated as emission sources. Star artifacts, planar resolution, spatial resolution, sensitivity, noise and contrast were evaluated using Fiji/ImageJ. The star artifact was most pronounced when the LEHR collimator was used, while the detector with the ME collimator showed no artifact due to its thicker septa. The detectors with the LEHR and LPHR collimators had higher planar resolution calculated using point source image data (FWHM = 8 ± 2 mm), while the detector with the ME collimator had the lowest planar resolution (FWHM = 13 ± 2 mm). Spatial resolution analysis using the Jaszczak phantom showed that the detector with the ME collimator had the lowest resolution (distance = 12.7 mm), while the detectors with the LEHR and LPHR collimators had higher spatial resolution (distance = 9.5 mm). Sensitivity was the highest for the detector with the ME collimator (112.6 cps/MBq), and the lowest for the detector with the LPHR collimator (59.3 cps/MBq). The noise was the lowest with the ME collimator, while the detector with the LPHR collimator provided the highest contrast.
In conclusion, the detectors with the LEHR and LPHR collimators showed higher planar and spatial resolution, making these collimators optimal for procedures requiring high precision in the image clarity. The detector with the LPHR collimator exhibited the highest contrast, which is advantageous for structure differentiation. The detector with the ME collimator provided the highest sensitivity and the lowest noise, which is beneficial for fast data acquisition or reduced patient applied activity and, consequently, absorbed dose. The detector with the LEHR collimator showed the most pronounced star artifact due to its thinner septa and was inferior to all others regarding sensitivity, contrast and noise.

[1] Morphis M, van Staden JA, du Raan H, Ljungberg M, Validation of a SIMIND Monte Carlo modelled gamma camera for Iodine-123 and Iodine-131 imaging, Heliyon, **7**, 1-11, (2021).
[2] Yuxin L; Choi E, Hayrapetian A, Appiah-Kubi E, Gershenson J, Asvadi NH, Berenji, GR, Comparison of Low-Energy and Medium-Energy Collimators for Thyroid Scintigraphy with 123I, Journal of Nuclear Medicine Technology, **50**, 25-29, (2022).

T26

Evaluation of HyperSight Cone-Beam CT for Adaptive Radiotherapy: A Comparison with Conventional CT and Previous Detector Generations

Christian Obwegs [1], **Wolfgang Sprengel,**[1,2] **Peter Winkler**[1,3]

1 Graz University of Technology,

2 Institute of Materials Physics, Graz University of Technology,

3 Department of Therapeutic Radiology and Oncology, Medical University of Graz, Austria

Objective:
The latest radiotherapy device at the Department of Therapeutic Radiology and Oncology in Graz features HyperSight technology, designed to enhance image quality. This study evaluates how closely Cone-Beam CT (CBCT) with HyperSight compares to conventional CT, assessing its potential use in radiation treatment planning and adaptive radiotherapy.

Materials and Methods:
A Gammex phantom with varying densities was used to evaluate the density-HU relationship. Calibration curves were generated for both the previous and new HyperSight detector using the filtered backprojection (FBP) and iterative CBCT reconstruction (iCBCT) algorithms, and conventional CT. Skull and pelvic phantoms were scanned, with line profiles extracted and converted into density values via calibration curves. Treatment plans (Hippocampus sparing brain irradiation and prostate plan) were created based on phantom images, and DVHs for different anatomical regions were analyzed. A Catphan phantom was also used to assess resolution, homogeneity, and noise, but these results are beyond the scope of this abstract.

Results:
For Hounsfield Unit (HU) values above 1000, deviations from conventional CT were observed for both the previous and the new detector generation. The analyzed dose-volume histograms (DVHs) for the planning target volumes (PTVs) and regions where radiation sparing is required showed statistical values (Median, D98.0%, and D2.0%) with no significant differences between the old and new detector generations. For the hippocampus sparing plan deviations using the iCBCT algorithm from the CT at the median were 0.1% with the old generation and 0.4% with HyperSight. In contrast, for the PTV, the median deviations were 0.4% with the old generation and 1.1% with HyperSight.

Conclusion:
Phantom measurements alone do not provide sufficient evidence to determine whether HyperSight offers a significant advantage over the previous detector generation in the context of adaptive radiotherapy. Further investigations involving patient imaging may yield more conclusive results, as the increased complexity and greater density variability in human anatomy could better reveal potential benefits of the new technology.

T27

Update of Italian diagnostic reference levels in interventional radiology

M. Cavallari [1], L. D'Ercole [1], R Padovani [2], C. Klersy [3], G Bernardi [4], G Campagnone[5], A Orlacchio [6], A Palma[7], S Grande[7], A Rosi [7]

[1] Struttura Complessa Fisica Sanitaria, Fondazione IRCCS Policlinico San Matteo, Pavia
[2] International Centre for Theoretical Physics, Trieste
[3] Biostatistica e Clinical Trial Center Direzione Scientifica Fondazione IRCCS Policlinico San Matteo, Pavia
[4] Associazione per la Ricerca in Cardiologia, Pordenone
[5] Formerly UO Fisica Sanitaria, AOU Bologna, Italy
[6] Dipartimento di Scienze Chirurgiche, Università degli Studi di Roma Tor Vergata – Radiologia DEA, Policlinico Universitario Tor Vergata, Roma
[7] Centro Nazionale delle Tecnologie Innovative in Sanità Pubblica, Istituto Superiore di Sanità, Roma

The transposition of Euratom Council Directive 2013/59 into Italian law (D. Lgs 101/2020) states that the Ministry of Health, through the Istituto Superiore di Sanità (ISS) and in collaboration with relevant scientific societies, promote the assessment and periodic review of Diagnostic Reference Levels (DRLs) for diagnostic radiology and interventional radiology procedures.
ISS is preparing an updated document for DRLs in interventional radiology [1,2], which will include the results of a national survey conducted between 2019 and 2022 by a Working Group (WG) led by ISS. The national survey was carried out in accordance with the European GDPR regulations adopted in 2018 and Italian law 101/2020. Fifty-three hospitals from across Italy participated in the survey.
The WG on DRLs identified the procedure types to be included in the survey from the categories most frequently performed in National Health Service (NHS) Centers, specifically those for which DRLs had been previously established in an earlier publication, in order to confirm or update these values:

- Hemodynamics: CA, CA + PTCA, TAVI
- Electrophysiology: pacemaker (single-chamber implantation, dual-chamber implantation, biventricular implantation), complex ablation with and without ElectroAnatomical Mapping (MEA), simple ablation with and without ElectroAnatomical Mapping (MEA)
- Vascular Body: TACE, EVAR, TIPS, PTA and/or stenting of carotid arteries and lower limbs
- Neurovascular: diagnostic cerebral angiography, cerebral aneurysm embolization, mechanical thrombectomy for ischemic stroke
- Extravascular: vertebroplasty, percutaneous biliary drainages and/or stenting, ERCP

New DRL values were derived for each of these procedures, except for TIPS, for which the standard value was used. For CA+PTCA, TACE, EVAR, cerebral angiography, cerebral aneurysm embolization, and mechanical thrombectomy, DRL values were also established according to the complexity of the procedure. For example for hemodynamic procedures the new DRL are: CA: 38 $Gycm^2$, 5 min and 473 mGy, CA+PTCA: 89 $Gycm^2$, 19 min and 1463 mGy, TAVI: 184 $Gycm^2$, 28 min and 1293 mGy.

[1] Padovani R, Compagnone G, D'Ercole L, Orlacchio A, Bernardi G, E. De Ponti, M.C. Marzola, S. Grande, A. Palma, F. Campanella, A. Rosi Livelli diagnostici di riferimento per la pratica nazionale di radiologia diagnostica e interventistica e di medicina nucleare diagnostica. Roma: Istituto Superiore di Sanità; 2020. Rapporti ISTISAN 20/22rev – aggiornamento del Rapporto ISTISAN 17/33

[2] D'Ercole L, Rosi A, Bernardi G, Compagnone G, Orlacchio A, Padovani R, Palma A and Grande S National survey to update the diagnostic reference levels in interventional radiology procedures in Italy: working methodology J. Radiol. Prot. 44 (2024) 011505

T28

Update of Italian diagnostic reference levels in interventional radiology

M. Cavallari [1], L. D'Ercole [1], R Padovani [2], C. Klersy [3], G Bernardi [4], G Campagnone[5], A Orlacchio [6], A Palma[7], S Grande[7], A Rosi [7]

[1] Struttura Complessa Fisica Sanitaria, Fondazione IRCCS Policlinico San Matteo, Pavia
[2] International Centre for Theoretical Physics, Trieste
[3] Biostatistica e Clinical Trial Center Direzione Scientifica Fondazione IRCCS Policlinico San Matteo, Pavia
[4] Associazione per la Ricerca in Cardiologia, Pordenone
[5] Formerly UO Fisica Sanitaria, AOU Bologna, Italy
[6] Dipartimento di Scienze Chirurgiche, Università degli Studi di Roma Tor Vergata – Radiologia DEA, Policlinico Universitario Tor Vergata, Roma
[7] Centro Nazionale delle Tecnologie Innovative in Sanità Pubblica, Istituto Superiore di Sanità, Roma

The transposition of Euratom Council Directive 2013/59 into Italian law (D. Lgs 101/2020) states that the Ministry of Health, through the Istituto Superiore di Sanità (ISS) and in collaboration with relevant scientific societies, promote the assessment and periodic review of Diagnostic Reference Levels (DRLs) for diagnostic radiology and interventional radiology procedures.
ISS is preparing an updated document for DRLs in interventional radiology [1,2], which will include the results of a national survey conducted between 2019 and 2022 by a Working Group (WG) led by ISS. The national survey was carried out in accordance with the European GDPR regulations adopted in 2018 and Italian law 101/2020. Fifty-three hospitals from across Italy participated in the survey.
The WG on DRLs identified the procedure types to be included in the survey from the categories most frequently performed in National Health Service (NHS) Centers, specifically those for which DRLs had been previously established in an earlier publication, in order to confirm or update these values:

- Hemodynamics: CA, CA + PTCA, TAVI
- Electrophysiology: pacemaker (single-chamber implantation, dual-chamber implantation, biventricular implantation), complex ablation with and without ElectroAnatomical Mapping (MEA), simple ablation with and without ElectroAnatomical Mapping (MEA)
- Vascular Body: TACE, EVAR, TIPS, PTA and/or stenting of carotid arteries and lower limbs
- Neurovascular: diagnostic cerebral angiography, cerebral aneurysm embolization, mechanical thrombectomy for ischemic stroke
- Extravascular: vertebroplasty, percutaneous biliary drainages and/or stenting, ERCP

New DRL values were derived for each of these procedures, except for TIPS, for which the standard value was used. For CA+PTCA, TACE, EVAR, cerebral angiography, cerebral aneurysm embolization, and mechanical thrombectomy, DRL values were also established according to the complexity of the procedure. For example for hemodynamic procedures the new DRL are: CA: 38 $Gycm^2$, 5 min and 473 mGy, CA+PTCA: 89 $Gycm^2$, 19 min and 1463 mGy, TAVI: 184 $Gycm^2$, 28 min and 1293 mGy.

[1] Padovani R, Compagnone G, D'Ercole L, Orlacchio A, Bernardi G, E. De Ponti, M.C. Marzola, S. Grande, A. Palma, F. Campanella, A. Rosi Livelli diagnostici di riferimento per la pratica nazionale di radiologia diagnostica e interventistica e di medicina nucleare diagnostica. Roma: Istituto Superiore di Sanità; 2020. Rapporti ISTISAN 20/22rev – aggiornamento del Rapporto ISTISAN 17/33

[2] D'Ercole L, Rosi A, Bernardi G, Compagnone G, Orlacchio A, Padovani R, Palma A and Grande S National survey to update the diagnostic reference levels in interventional radiology procedures in Italy: working methodology J. Radiol. Prot. 44 (2024) 011505

T29

Monte Carlo analysis of dose deposition by alpha emitters in Targeted Radionuclide Therapy

L. Palenciano-Castro[1] **and M. Anguiano**[1]

[1]*Department of Atomic, Molecular and Nuclear Physics, University of Granada (Spain)*

Targeted Radionuclide Therapy (TRT) for cancer typically employs β^- electron emitters such as ^{131}I, ^{90}Y or ^{177}Lu [1]. However, low-energy alpha particles (3-10 MeV) exhibit a shorter range in matter compared to β^- electrons, along with a higher Linear Energy Transfer (LET). This results in a more localized dose deposition within the tumor and increased effective damage. Consequently, alpha-emitting radionuclides have emerged as promising candidates for TRT treatments [2].

To optimize and improve these therapies, it is essential to perform microdosimetric studies to analyze dose deposition at the cellular level. Monte Carlo methods are a powerful tool in this context, since they allow a detailed description of radiation transport and interactions with matter.

In this work, we compare the performance of different Monte Carlo codes for simulating the transport of low-energy alpha particles, to analyze the impact of the underlying physical models used for describing alpha-matter interactions in the simulation results. Additionally, we study how the choice of radionuclide influences dose deposition in TRT treatments.

To this end, we calculate dose deposition in a simplified cell model using a monoenergetic alpha source, employing the Monte Carlo codes PENHAN [3] and FLUKA [4]. Furthermore, we perform simulations using various alpha emitters that show suitable features for TRT, such as ^{211}At or ^{225}Ac [5], focusing on the dose deposited within the cell nucleus when the radioisotope is distributed within the cell.

Although PENHAN and FLUKA yield similar results, some discrepancies arise, highlighting the influence of the implemented physical models and transport algorithms on the simulation results. Additionally, our results show significant differences in dose deposition between emitters, underscoring the importance of selecting the most adequate radionuclide for each specific clinical scenario.

This study emphasizes the need for careful validation of the physical models employed in Monte Carlo simulations, as they directly influence the accuracy of results which are used to improve the radiotherapy techniques. Moreover, our findings further highlight the importance of detailed dosimetric studies when designing TRT treatments, ensuring optimization of the treatment efficacy while minimizing damage to healthy tissues.

[1] S. Salih et al. Radiopharmaceutical Treatments for Cancer Therapy, Radionuclides Characteristics, Applications, and Challenges. Molecules **27** (2022).

[2] S. Tronchin et al. Dosimetry in targeted alpha therapy. A systematic review: current findings and what is needed. Physics in Medicine & Biology **67** (2022).

[3] F. Salvat. PENHAN-2024: Monte Carlo simulation of the coupled transport of electrons, photons, nucleons, and alphas. Issy-les-Molineaux, France: Nuclear Energy Agency (2024).

[4] A. Ferrari et al. FLUKA: A multi-particle transport code. SLAC-R-773 (2005).

[5] A. Jang et al. Targeted Alpha-Particle Therapy: A Review of Current Trials. International Journal of Molecular Sciences **24** (2023).

T30

Metal implants, gas pockets, and intra-venous contrast – should automatic CT-ED conversion be trusted?

Primož Peterlin, Aljaša Jenko, Matevž Mlekuž, and Rihard Hudej

Institute of Oncology Ljubljana, Zaloška 2, Ljubljana, Slovenia

Background. Computed tomogram (CT) serves a double role in radiation oncology, providing anatomical structural information on one hand, and serving as a three dimensional distribution of electron density (ED) – which is subsequently used for dose calculation – on the other. There are however a few cases where the ED information in the CT scans is either not reliable or does not accurately represent the tissue properties: metal artefacts, gas pockets, and intravenous contrast. This paper presents an overview of handling these issues at the authors' institution.

Materials and methods. The mechanisms behind the three effects is different. Metal implants (hip implants, dental fillings, etc.) are present both during taking the planning CT and during the treatment; however the artefacts affect both the imaged shape and size of metal implants and their electron density. Metal artefact reduction algorithms mitigate the artifacts, but also affect the estimated electron density of the implant [1]. Gas pockets in the bowel are imaged correctly at the time of taking the planning CT, however their location may be different at treatment time, or may not be present at all. Similarly, intravenous contrast is only present at taking the planning CT, and not later at treatment.

Results. At our clinic, *metal implants* are handled differently with regard to the bit depth of CT scans. On CT-scans with 12-bit depth (-1024–3071 HU), pixel values reach saturation in/around the artefact, and accurate delineation of the artefact is challenging. Planners must make an educated guess with regard to the correct shape of the implant, delineate it and assigned a value of ED of either stainless steel or titanium. On CT-scans with 16-bit depth, the ED is preserved and not overridden. Metal implants are also avoided on the entry side of the beam. There is no consensus on handling *air pockets*; some planners contour them and assign them the ED value of water, others leave them unmodified. When using intensity-modulated radiotherapy (IMRT) or volumetric modulated arc therapy (VMAT), it is however advisable to assign them a non-zero ED in cases where the planning target volume (PTV) overlaps with an air pocket. *Intravenous contrast* is contoured in the vicinity of the target and assigned the ED of either water or blood/muscle tissue. Taking two CT sets (with and without intravenous contrast) is not considered necessary.

Discussion. The debate on the clinical impact of the CT artefacts has been going on for decades. While most studies, both early [2] and recent [3] dismiss the dosimetric effect of the intravenous contrast as insignificant (below 2%), some studies [4] report cases in which it led to a 8% change in dose. A recent study dealing with gas pockets [5] has found overriding ED in gas pockets with their average value superior to overriding it with either air or water ED.

Conclusion. Lacking international or national recommendations, planners are left to their own devices, which opens a possibility of either inducing important dosimetric discrepancies, or contrary, wasting time and resources on a dosimetrically insignificant effect. Producing some sort of guidelines therefore seems a worthwhile effort.

[1] D. Giantsoudi et al., Phys. Med. Biol. **62**, R49 (2017).
[2] S. J. Liauw et al., Am. J. Clin. Oncol. **28**, 456 (2005).
[3] A. A. Elawadi et al., Appl. Sci. **11**, 8355 (2021).
[4] H. J. Kim et al., Radiat. Oncol. **8**, 244 (2013).
[5] M. Nardini et al., Front. Oncol. **13**, 1280836 (2023).

T31

Intercomparison of calibration factor of ionizing chambers in clinical practise

Veljko Petrović [1], Katarina Bito[1], Miloš Jonić[1]

[1] *University Clinical Center Niš, Niš, Serbia*

Introduction

For dosimetry purposes, cylindrical ionizing chambers are the most commonly used. Therefore, it is of utmost importance to regularly calibrate the chambers that are in practical use. This is performed by second standard dosimetry laboratories (SSDL), and it is mandated to be done every two years. However, chambers can be damaged sometimes, due to poor handling or conditions in which they are kept. If there is suspicion that something might be wrong with the chamber, it is good practise to check it with some other chambers that is not being used regularly, which is kept safe and whose calibration factor is measured by SSDL. This process is called intercomparison. The idea behind this small study is to check viability of intercomparison performed in clinical surroundings with readily available equipment.

Materials and Methods

For this study, all the measurements were performed in SP34 phantom. The phantom factor played no effect on measurement, since all that was needed was relation of measured signals for individual chambers under the same conditions: SSD 100 *cm*, depth 10 *cm*, 100 *MU*, and with energy of 6 *MV*. Use of SP34 was decided because of efficiency. Firstly, set of 5 measurements was performed with reference chamber, which was most recently calibrated. Then, the chambers were swapped, and the process was repeated for 4 chambers that were used in the study. Measured signals were then compared to reference chamber.

Results and discussion

All the measured signals were compared to reference chamber, one by one, then the mean value of these relations was used to determine individual correction factors, which were then compared to factors provided by SSDL. The results are represented in Table 1. As can be seen, measured factors are in grate agreement with the ones determined by SSDL. Deviation being less than 1% for all the chambers is proof that intercomparison in clinical practice is a valid tool for checking the suitability of chambers.

Serial No. of the chamber	Measured cal. Factor	Cal. Factor from SSDL	Deviation (%)
3904	48,22±0,05	48,25±0,56	-0,06
1740	47,85±0,04	47,80±0,55	0,10
1741	47,44±0,05	47,48±0,61	-0,08
0812	47,77±0,01	47,71±0,58	0,13

Table 1: Intercomparison results

References

[1] IAEA (2024). Absorbed Dose Determination in External Beam Radiotherapy. Vienna: Inernational Atomic Energy Agency

[2] Veljko Petrovic (2024), Intercomparison of Ionization Chamber Calibration Factor Using SP34 Phantom, Niš

T32

Impact of knowledge-based treatment planning on adaptive radiotherapy for prostate cancer

Tamás Pócza[1,2], András Herein[1], Csilla Pesznyák[1,2], Zoltán Takácsi-Nagy[1,3], Tibor Major[1,3]

[1]*National Institute of Oncology, Centre of Radiotherapy, Budapest*
[2]*Budapest University of Technology and Economics, Institute of Nuclear Techniques*
[3]*Semmelweis University, Department of Oncology*

Knowledge-based treatment planning (KBTP) plays an important role in prostate cancer treatment planning. KBTP models can also be applied in online adaptive radiation therapy. The goal of this study was to examine the performance of a model for the adaptive workflow.

Ten locally advanced prostate tumour patients were previously treated in 28 fractions with a simultaneous integrated boost technique: 2.5 Gy for the prostate gland (PROS), 2.1 Gy for the proximal part of the seminal vesicles (PVS), and 1.8 Gy for the pelvic lymph nodes (LN) [1]. Treatment planning was performed in Varian Eclipse treatment planning system (Varian Medical Systems, Palo Alto, CA) using a locally developed RapidPlan (RP) (Varian Medical Systems, Palo Alto, CA) KBTP model based on 50 patients. Besides the original (Eclipse) plans, alternative plans were created for these patients using the Varian Ethos (Varian Medical Systems, Palo Alto, CA) treatment planning system, with (Ethos+RP) or without (Ethos) KBTP. The dosimetric parameters of plans with Eclipse, Ethos, and Ethos+RP techniques were analyzed. The dose parameters of bladder, rectum, femoral heads BODY and the target volume were evaluated. The necessary number of monitor units (MU) was also collected.

For the LN, PVS, and PROS target volumes, the average V95% parameters were as follows: 98.2%, 99.7%, and 99.9% with Eclipse; 99.9%, 100%, and 99.9% with Ethos+RP; and 99.9%, 100%, and 99.8% with Ethos, respectively. The differences in dose coverage parameters for the PVS target were negligible. The dosimetric parameters of the rectum and bladder were significantly more favorable for Eclipse plans, as shown in *Figure 1*. The mean dose values of the BODY were 11.5 Gy, 12.4 Gy, and 11.9 Gy for Eclipse, Ethos, and Ethos+RP techniques, respectively. The average numbers of monitor units were 1062 MU for Eclipse, 1003 MU for Ethos, and 1154 MU for Ethos+RP plans.

Technique	Rectum Dmean (Gy)	Rectum V45.45Gy (%)	Rectum V63.63Gy (%)	Bladder Dmean (Gy)	Bladder V54.54Gy (%)	Bladder V63.63Gy (%)
Eclipse	**32.1**	**26.3**	**10.4**	**32.7**	**12.5**	**6.2**
Ethos	**44.9**	**42.4**	**11.8**	**42.4**	**14.4**	**6.1**
Ethos+RP	**36.6**	**31.7**	**11.2**	**35.3**	**13.1**	**6.0**

***Figure 1**: Dosimetric parameters of the rectum and bladder with different techniques.*

The study highlights key differences in dosimetric outcomes between Eclipse, Ethos, and Ethos+RP techniques. The applied technique affects on the dosimetric parameters, such as bladder and rectum doses, which are varied significantly. KBTP models based on standard plans should be carefully applied in adaptive planning.

References:

[1] Jorgo K, Polgar C, Major T, Stelczer G, Herein A, Pocza T, Gesztesi L, Agoston P. Acute and Late Toxicity after Moderate Hypofractionation with Simultaneous Integrated Boost (SIB) Radiation Therapy for Prostate Cancer. A Single Institution, Prospective Study. Pathol Oncol Res. 2020 Apr;26(2):905-912

T33

Comparative Dosimetric Analysis of Varian Halcyon and TrueBeam Platforms for Rectum and Inguinal Irradiation

Una Popović [1] , Laza Rutonjski [1] Ozren Čudić[1], Milana Vezirović[1,2], Borislava Petrović [1,2]

[1]Oncology Institute Vojvodina, Sremska Kamenica, Serbia
[2] Faculty of Sciences, University Novi Sad, Novi Sad, Serbia

Background: The treatment of anatomically complex targets, such as the rectum and inguinal regions, presents unique challenges in radiotherapy planning. In this study the dosimetric performance of two linear accelerators, Varian Halcyon™ and Varian TrueBeam™, in delivering volumetric modulated arc therapy (VMAT) plans for these regions, were compared.

Methods: Treatment plans were generated for both platforms using identical prescription doses and the volume receiving 90%, 80%, 70%, 60%, 50%, and 40% of the prescribed dose were recognised, analyzed and compared.

Results and discussion: The analysis revealed that Halcyon plans delivered higher doses to normal tissues compared to TrueBeam plans at all evaluated dose levels. The average volume differences across dose levels were significantly greater for Halcyon. Key differences in dose delivery were attributed to the inability of Halcyon to adjust jaw positions manually, therefore open MLC configurations can increase dose spillage. These findings highlight the superior ability of TrueBeam's adjustable jaws and MLC system to achieve sharper dose gradients and minimize exposure to surrounding tissues.

Conclusion: While both platforms are capable of delivering clinically acceptable plans, TrueBeam demonstrates superior dosimetric performance for anatomically complex targets due to its beam-shaping capabilities, and the fixed jaw setting on the Halcyon is seen as a limitation in protecting healthy tissue. This study provides a simple insight into how technical differences can affect treatment plans. These findings may help guide clinicians and medical physicists when choosing the best machine and settings for each patient, ensuring treatments are both safe and effective.

Literature:

- [1] Li T, Scheuermann R, Lin A, Teo BK, Zou W, Swisher-McClure S, Alonso-Basanta M, Lukens JN, Fotouhi Ghiam A, Kennedy C, Kim MM, Mihailidis D, Metz JM, Dong L. Impact of Multi-leaf Collimator Parameters on Head and Neck Plan Quality and Delivery: A Comparison between Halcyon™ and Truebeam® Treatment Delivery Systems. Cureus. 2018 Nov 28;10(11):e3648. doi: 10.7759/cureus.3648. PMID: 30723647; PMCID: PMC6351111.

- [2] Zhu Qizhen, Yang Bo, Wang Zhiqun, et al. A comprehensive comparison of dosimetric quality and complexity of multi-site VMAT plans based on Halcyon 2.0 and Truebeam[J]. Chinese Journal of Radiation Oncology, 2023, 32(03): 241-247. DOI: 10.3760/cma.j.cn113030-20211108-00456

T34

Abstract for the oral presentation

Evaluation of Monte-Carlo-based Iterative SPECT Reconstruction: anthropomorphic phantom study

Ivan Pribanić[1,2], Michael Ljungberg[3], Slaven Jurković[1,2]

[1] Medical Physics and Radiation Protection Department, University Hospital Rijeka, Croatia.
[2]Department of Medical Physics and Biophysics, Faculty of Medicine, University of Rijeka, Croatia.
[3]Department of Medical Radiation Physics, Lund University, Lund, Sweden.

Monte Carlo iterative reconstruction (MCIR) algorithm SIMREC may generate images of superior quality compared to standard reconstruction algorithms [1,2]. The aim of this research is to further evaluate the SIMREC using anthropomorphic Kyoto thorax phantom. The goal is to optimize reconstruction parameters in convergence of contrast study while also investigating the accuracy of activity calculation and contrast recovery in SIMREC reconstructed image data.

The anthropomorphic Kyoto thorax phantom was used to simulate ^{99m}Tc-EDDA/HYNIC-TOC biodistribution in case of single liver lesion. A 3D-printed spheres of volume 11.5 ml and 5.5 ml were used to simulate a lesion. It was not feasible to insert such large objects directly into phantom's liver. Therefore, two image datasets were created: a phantom with a sphere positioned in the phantom's liver without other phantom organs and a phantom with all phantom organs. Both datasets were registered and merged using software written in python. Phantom was imaged using Siemens Symbia Intevo SPECT/CT system with dual-energy window. Scatter correction and CT attenuation correction were performed. For both spheres, imaging was performed for phantom lesion to liver activity concentration ratios ranging from approximately 2 to 27. A low-noise image dataset acquired with longer acquisition time was used for partial volume correction. Image datasets were reconstructed using SIMREC and Siemens Flash3D clinical iterative reconstruction algorithm (CIR). Reconstruction was performed for up to 20 iterations, while number of subsets was set to 45 for CIR and 20 subsets were used with 9 projections per subset for SIMREC. Image data were analysed using a software written in python. Hot-sphere contrast, contrast-to-noise ratio, ratio of sphere counts to sphere activity with and without partial volume corrections and sphere counts normalized to sphere counts for maximum number of iterations were plotted against number of iterations and analysed for both SIMREC and CIR.

Results indicate SIMREC was able to achieve contrast convergence after small number of iterations. Activity recovered from sphere ROIs was within 10% of true value. CIR required larger number of iterations to achieve convergence with low accuracy of activity determination even when sensitivity calibration procedure with uniform cylindrical phantom was performed before. Results clearly indicate the potential of SIMREC Monte Carlo reconstruction algorithm for providing reconstructed image datasets of better quality than CIR with correct contrast and activity values.

[1] Michael Ljungberg and Sven-Erik Strand. A Monte Carlo program for the simulation of scintillation camera characteristics. Comput Methods Programs Biomed 1989 29:4;257-72.

[2] Johan Gustafsson, Gustav Brolin, and Michael Ljungberg. Monte Carlo-based SPECT reconstruction within the SIMIND framework. Phys Med Biol 2018 63:24; 245012.

T35

Breast Density Patterns and their Relationship with Breast Cancer among a Large Cohort of Ghanaian Women

Caroline Kachana Pwamang[1,2], Edem Sosu[1,3], Francis Hasford[1,3], Mary Boadu[1,3], Klenam Dzefi-Tettey[4,5], Renata Longo[6].

[1]*University of Ghana, School of Nuclear and Allied Sciences, Medical Physics Department, Accra, Ghana*
[2]*Radiological and Non-Ionizing Installations Directorate, Nuclear Regulatory Authority, Accra, Ghana*
[3]*Radiological and Medical Science Research Institute, Ghana Atomic Energy Commission, Accra, Ghana.*
[4]*Radiology Department, Korle Bu Teaching Hospital, Accra, Ghana*
[5]*Department of Radiology, University of Health and Allied Sciences, Ho, Ghana.*
[6]*University of Trieste, Department of Physics, Trieste, Italy.*

Background: Breast cancer is a significant global health challenge, with Africa and other developing countries experiencing its greatest impact. Gaining deeper insights into breast density (an independent risk factor) and its correlation with breast cancer is essential for improving early detection and management. However, such data are scarce across Africa and non-existent in Ghana.
Aim: To investigate the relationship between breast density and cancer incidence among study participants in Ghana.
Methodology: A retrospective cross-sectional study was undertaken among 2,108 women who underwent mammography examinations at the Korle Bu Teaching Hospital from October 2011 to December 2022. Breast density patterns were obtained from anonymised patient records and evaluated via visual assessment by Radiologists using the American College of Radiology (ACR) Breast Imaging-Reporting and Data System (BI-RADS) criteria.
Results: Breast density classes A (almost entirely fatty) and B (scattered fibroglandular tissues) were more than C (heterogeneously dense breasts) and D (extremely dense breasts). Class B (44%, n = 935) was the main pattern in the study population, followed by class A (39%, n = 821). Class C recorded 16% (n = 397), while Class D was the least recorded (1%, n = 23). Over 50% of all the breast density types recorded benign findings (BI-RADS 2), while less than 10% recorded negative findings (BI-RADS 1). For breast density type A, 6% of participants had probably benign findings (BI-RADS 3), 6% had BI-RADS 4 findings (suspicious of malignancy), and 6% had BI-RADS 5 findings (highly suggestive of malignancy). Among those with B-type breasts, 9% had BI-RADS 3, 7% had BI-RADS 4, and 8% had BI-RADS 5. Participants with C-type breast density had 11% BI-RADS 3, 10% had BI-RADS 4, and 10% had BI-RADS 5. For those with D-type breast density, 17% had BI-RADS 3, 17% had BI-RADS 4, and 13% had BI-RADS 5. 1% of breast density types A, B, and C had confirmed breast cancer (BI-RADS 6). There is a trend of increasing BI-RADS 3, BI-RADS 4, and BI-RADS 5 with higher breast density, suggesting that participants with denser breasts may have a higher likelihood of suspicious or malignant findings. From Fisher's Exact Test, $p < 0.05$. There is a significant relationship between breast density type and breast cancer. Also, there is a significant relationship between age and breast density type $p < 0.05$.
Conclusion: There is a significant association between breast density and cancer diagnosis, with lower breast density observed in older women, a finding that aligns with published studies.

References

[1] Checka CM, Chun JE, Schnabel FR, Lee J, Toth H. Am J Roentgenol. The relationship of mammographic density and age: implications for breast cancer screening. 198(3): W292–5 (2012).
[2] Gathara J, Galukande M, Kiguli-Malwadde E. East Cent Afr J Surg. Breast density as a risk factor for breast cancer amongst a cohort of women in Uganda. 17: 98–103 (2012).
[3] Obajimi, M. O., Adeniji-Sofoluwe, A. T. S., Oluwasola, A. O., Adedokun, B. O., Soyemi, T. O., Olopade, F., & Newstead, G. Breast disease. Mammographic breast pattern in Nigerian women in Ibadan, Nigeria. 33(1), 9-15 (2012).
[4] Sung, H., Ferlay, J., Siegel, R. L., Laversanne, M., Soerjomataram, I., Jemal, A., & Bray, F. CA: a cancer journal for clinicians. Global cancer statistics 2020: GLOBOCAN estimates of incidence and mortality worldwide for 36 cancers in 185 countries. 71(3), 209-249 (2021).
[5] Kocer, H. B., Menekse, E., Turan, U., Namdaroglu, O., Barca, A. N., Araz, L., ... & Bozkurt, B. The Medical Bulletin of Sisli Etfal Hospital. The relationship between mammographic density and factors affecting breast cancer risk. 56(1), 119-125 (2022).

T36

Evaluation of a New Multi-Energy QA Phantom for Spectral CT: Optimizing Diagnostic Imaging with Virtual Monochromatic Imaging and Metal Artifact Reduction

Michèle-Louise Regner [1,2] , Lilian Abou Assali [1,2] , Andreas Mahnken [2] and Martin Fiebich [1,2]

[1]Department of Medical Physics and Radiation Protection (IMPS), University of Applied Sciences Mittelhessen, Gießen, Germany
[2] Department of Diagnostic and Interventional Radiology, University Hospital Gießen-Marburg (UKGM), Marburg, Germany

Spectral computed tomography (CT) enables a more quantitative evaluation of clinical imaging data, providing greater accuracy and diagnostic precision. Advanced quantitative imaging techniques, including virtual monochromatic imaging (VMI) and iodine quantification (IQ) have become essential diagnostic tools for tumor characterization and tissue differentiation, enhancing clinical decision-making [1, 2]. An additional advantage of using VMIs is their ability to reduce metal artifacts, caused by metallic implants such as hip prostheses. These implants often result in photon starvation and beam hardening, severely limiting diagnostic accuracy [3].

In this study, we present a newly introduced multi-energy QA phantom (QRM, PTW, Germany) with various inserts, which was scanned at different dose levels. VMIs from 40 keV to 190 keV were reconstructed and analyzed to assess different iodine concentration tubes. Additionally, a metal implant was simulated by placing an iron needle into a water-filled insert within the phantom and the effectiveness of spectral CT monoenergetic imaging in combination with iterative metal artifact reduction algorithm (iMAR) was evaluated. Four types of CT images were compared: conventional CT, CT with iMAR, VMI, and VMI with iMAR.

Our results demonstrate that VMIs, provide superior signal-to-noise ratio (SNR) and contrast-to-noise ratio (CNR) in comparison to linear-blended images (LBIs). Among the VMIs, the 70 keV image shows the best overall image quality. Furthermore, at all dose levels, VMIs showed a marked potential for contrast medium reduction, outperforming both traditional LBIs and single-energy CT in terms of image quality and contrast enhancement. These findings emphasize the potential of the new multi-energy QA phantom and VMIs as powerful tools for optimizing diagnostic imaging, enabling reduced radiation exposure and contrast agent use, while maintaining high image quality. Furthermore, the combination of monoenergetic imaging and iMAR resulted in the most substantial reduction in metal artifacts, improving the visualization of surrounding structures. These findings suggest that VMI + iMARs reconstruction provides a superior approach for enhancing diagnostic quality in patients with metallic implants.

[1] D. Cester et al., *Quantitative imaging in medicine and surgery*, vol. 12, pp. 726–741 (2022).
[2] S. Vrbaski et al., *Medical physics*, vol. 50, pp. 5421–5433 (2023).
[3] M. Selles et al., *European journal of radiology*, vol. 170, p. 111276 (2024).

T37

Radiation Exposure of Interventional Pain Physicians

Jelena Samac [1,2,4] , Predrag Bozovic [3] , Jelena Stanković Petrović[3] and Borislava Petrovic [4,5]

[1] 1Faculty of Medicine, University of Novi Sad, Serbia; [2] University Clinical Centre of Vojvodina, Novi Sad, Serbia; [3] Vinca Institute of Nuclear Sciences, University of Belgrade, Serbia; [4] Faculty of Sciences, University of Novi Sad Novi Sad, Serbia; [5] Oncology Institute of Vojvodina, Sremska Kamenica, Serbia

Introduction: Fluoroscopy is used in pain management procedures, performed by anaesthesiologists, for assuring correct needle placement and accurate delivery of injected drug. Needle manipulation requires operator to be in close proximity to the patient and hence source of radiation. The practice being new in our institution, the aim of this study was to investigate operator's exposure per procedure and to assess the need for future monitoring.
Methods: Each operator was assigned 5 thermoluminescent dosimeters (TLD), three placed on a forehead to determine eye lens dose distribution, calibrated in terms of Hp(0.03), one over and one under protective apron, calibrated in terms of Hp(10). 3 operators involved performed a total of 16 procedures during study period.
Results: The dose for left and right eye, expressed as mean (max, min) median, was 145 (258, 103) 131 μSv and 140 (265, 103) 119 μSv, respectfully, while under and over apron dose was found to be 58 (80, 40) 57 μSv and 77 (186, 46) 64 μSv, respectfully, per procedure. Accounting for maximum number of patients per week to be 5 in current practice, expected annual eye lens and whole body dose could be estimated as a) 35,5 and 19.25 mSv, or b) 61.5 and 46,5 mSv, based on a) mean dose per procedure or b) highest recorded dose.
Discussion: The results in this paper are comparable with data available in recent literature [1, 2]. Exposure of both eyes could be considered as the same. Estimated annual dose does not encounter for the use of protective glasses or aprons, indicating that actual dose received by the eyes and body are lower. Additionally, they assume one operator is performing all procedures, whereas the actual workload is divided between several operators. However, these results do show that not wearing personal protective equipment leaves a possibility of reaching an annual dose limit set by ICRP of 20 mSv for eyes and 50 mSv for the body. In that case, one operator could perform only 3 procedures per week before reaching annual dose limit for eyes. Maximum recorded values all correspond to one case, where ceiling suspended protective screen was not used, highlighting the importance of use of all available radiation protection equipment, supported by the literature [3, 4]. Raising awareness among operators regarding radiation protection as well as radiation safety education can effectively reduce radiation exposure [5].
Conclusion: Future monitoring is needed, particularly if a workload is to be increased.

[1] Nguyen D, Piché F, Mares C, Denis I. Radiation exposure in fluoroscopy guided spinal interventions: A prospective observational study of standard practice in a physiatry academic center. Interv Pain Med. 2(3):100273 (2023)
[2] Zhitny VP, Do K, Kawana E, Do J, Wajda MC, Gualtier RT, Goodman AJ, Zou S. Radiation Exposure in Interventional Pain Management Physicians: A Systematic Review of the Current Literature. Pain Physician. (1):E17-E35 (2024)
[3] Park S, Kim M, Kim JH. Radiation safety for pain physicians: principles and recommendations. Korean J Pain. 35(2):129-139 (2022)
[4] Nicol AL, Benzon HT, Liu BP. Radiation Exposure in Interventional Pain Management> We Still Have Much to Learn. Pain Practice. 15(5):389-392 (2015)
[5] Slegers AS, Gültuna I, Aukes JA, van Gorp EJ, Blommers FM, Niehof SP, Bosman J. Coaching Reduced the Radiation Dose of Pain Physicians by Half during Interventional Procedures. Pain Pract. 15(5):400-6 (2015)

T38

Monitoring of Indoor Air Quality to Prevent diffusion of Infection Diseases and improve Occupants' Safeguards

B. Santoro[1,2]

[1] *Department of Physics, University of Trieste, Trieste*

[2] *Department of Physics and Astronomy "Galileo Galilei", University of Padua, Padua*

Air quality significantly impacts human health. Poor air quality has been linked to symptoms such as headaches and more severe manifestations, including dizziness and tachycardia [1]. Furthermore, exposure to high levels of pollutants has been shown to reduce cognitive abilities [2]. Finally, enclosed environments are recognized as high-risk areas for the spread of infections, as demonstrated during the COVID-19 pandemic.
Since people spent 90% of their time indoor - at home, school or the offices - monitoring of air quality in these environments is fundamental to improve occupants' health [3].
To address this, I propose a joint software-hardware system to easily evaluate indoor air quality and risk of infection. The system monitors key indoor air quality proxies, including carbon dioxide (CO_2), temperature, pressure, and relative humidity, using four selected sensors.
Firstly, a Graphical User Interface (GUI) was developed in Python to acquire data from sensors, display it in real-time, and store it for further analysis. The software-hardware combination was tested in one of the offices of the University of Trieste to evaluate software performances, stability and check measurements' reliability. The software was also improved by adding a calculator of infection probability from airborne pathogens such as influenza, tuberculosis and SARS-CoV-2.
Following the testing period, the sensors and tool were distributed to students and Hospital personnel to sample other environments of interest with potential risk of infection. Data were collected in two classrooms of the University of Trieste, a patients' room of the Internal Medicine Department and two locals of the Pathology Department of the University Hospital of Trieste.
During the office testing period, environmental data were analyzed to identify daily and seasonal patterns. CO_2 measurements were clustered according to air quality levels using a machine-learning-based clustering method in Python. The clustering results were validated using both internal and external metrics, comparing the clusters with indoor air quality classifications from international agencies [4, 5]. Although data from other environments were more limited due to availability constraints, they provided valuable insights into the characterization of different indoor spaces in terms of air quality.

[1] S. D. Lowther, S. Dimitroulopoulou, K. Foxal, et al. Low Level Carbon Dioxide Indoors—A Pollution Indicator or a Pollutant? A Health-Based Perspective. Environments **8(11)**, 125 (2021)
[2] Y. Fan, X. Cao , J. Zhang , et al. Short-term exposure to indoor carbon dioxide and cognitive task performance: A systematic review and meta-analysis. Build. Environ., **237** (2023).
[3] A. C. Lewis, D. Jenkins, C. J. M. Whitty, et al. Hidden harms of indoor air pollution - five steps to expose them. Nat. **614**, 220-223 (2023).
[4] Refrigerating American Society of Heating and Air-Conditioning Engineers. ASHRAE Position Document on Indoor Carbon Dioxide. 2022.
[5] Ente Italiano di Normazione. Prestazione energetica degli edifici - Ventilazione per gli edifici - Parte 1: Parametri di ingresso dell'ambiente interno per la progettazione e la valutazione della prestazione energetica degli edifici in relazione alla qualità dell'aria interna, all'ambiente termico, all'illuminazione e all'acustica. UNI EN 16798-1. 2019.

T39

Measurement of PDDs for the Xstrahl 200 orthovoltage therapy machine using the PTW Advanced Markus chamber

A. Sarvari [1], P. Peterlin[1] and B. Brojan [1]

[1](Institute of Oncology Ljubljana)

At the Institute of Oncology Ljubljana, a kilovoltage treatment device, Xstrahl 200 (Xstrahl Ltd), is used to treat superficial lesions and skin cancer. The unit produces X-rays in the kilovolt range from 40 kV up to 220 kV. The unit comes equipped with two types of applicators: round and square-shaped. Round applicators (diameters from 3 cm to 10 cm) are open and have a 30 cm FSD, while the square ones (field sizes from 4 × 4 cm² to 20 × 20 cm²) are closed with a 50 cm FSD. In this study, we measured the percentage depth dose (PDD) curves using the Advanced Markus chamber (PTW type 34045) for each available energy and applicator. Measurements were performed in the Blue Phantom² 3D scanning phantom (IBA Dosimetry GmbH) using the myQA Accept (8.5.21.0) scanning software (IBA Dosimetry GmbH). To avoid any collision with the measuring equipment, we performed the measurements at 31 cm FSD for round applicators and 51 cm FSD for square applicators. For the largest round applicator (10 cm), additional measurements were performed at an FSD of 30 cm. Point-step scans were conducted from a depth of 50 mm to the surface, as we were only interested in shallow depths. From 50 mm to 10 mm depth, a 1 mm increment scan step was used, while from 10 mm to 0 mm depth, a 0.5 mm increment scan step was applied. The step mode was used in order to decrease water sufrace fluctuations during measurement. Reference chamber was not used. Prior to the PDD measurements, CAX correction was performed, including inline and crossline profile scans at two different depths, in order to determine any beam inclination and centre displacement. By applying the correction, we ensured that the scan was conducted along the central axis of the applicator, which was particularly important for small-sized applicators. All measurements were smoothed and rescaled to 100% at dmax. These measurements are in good agreement with the data from the literature.

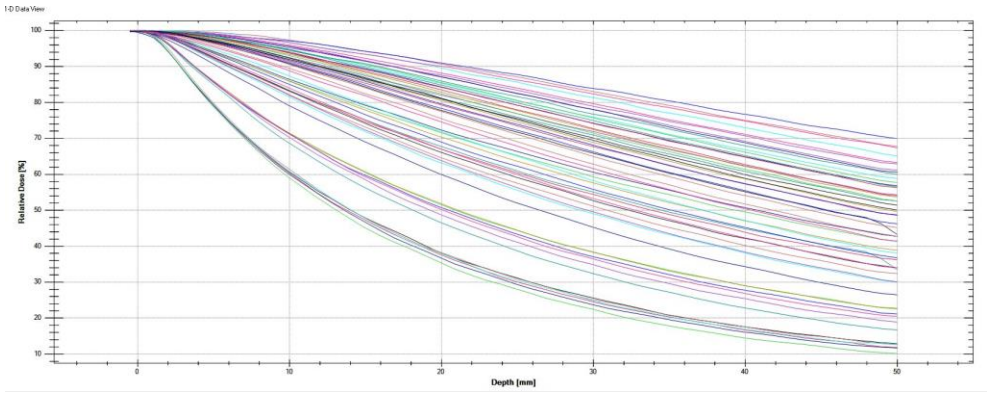

Figure 1: Depth dose curves for different energies and different round applicators

[1] Aird EGA, Burns JE, Day MJ, Duane S, Jordan TJ, Kacperek A et al (1996) Central Axis Depth Dose Data for Use in Radiotherapy. British Journal of Radiology Suppl 25. London: The British Institute of Radiology.

[2] Ma C, Coffey C, DeWerd L, Liu C, Nath R, Seltzer S, Seuntjens J (2001), AAPM Protocol for 40-300 Kv X-Ray Beam Dosimetry in Radiotherapy and Radiobiology, Med Phys 28:868-893.

T40

Acceptance testing and initial performance evaluation of the ARTIS Pheno C-arm system at Cattinara Hospital, Italy

Sara Savatović[1], Benedetta Santoro[1], Michele Signoriello[2], Sandro Lepidi[3], Mara Severgnini[2], and Paola Bregant[2]

[1] *Department of Physics and Astronomy "Galileo Galilei", University of Padua, 35131 Padua, Italy;*
[2] *Department of Medical Physics, Azienda Sanitaria Universitaria Giuliano-Isontina (ASUGI), 34129 Trieste, Italy;*
[3] *Division of Vascular and Endovascular Surgery, Department of Clinical Surgical and Health Sciences, University of Trieste, 34149 Trieste, Italy;*

A hybrid operating room is an advanced surgical environment that integrates state-of-the-art medical imaging systems, enabling real-time image guidance for complex interventional procedures alongside equipment for standard surgical interventions, such as cardiovascular and neurological ones. Cattinara Hospital in Trieste, Italy, recently installed a new C-arm system, the ARTIS Pheno (Siemens Healthcare GmbH, Forchheim, Germany), designed to support advanced interventional procedures. This work presents the initial acceptance tests, focusing on the functionality of the fluoroscopic Automatic Dose Rate Control (ADRC) and image quality control logic, evaluating its performance and potential challenges.

The AAPM Report No. 125 [1] serves as a key reference for ADRC in angiographic systems, particularly regarding spectral shaping filters and exposure parameters variation. However, since its publication, significant technological advancements have led to the development of new ADRC systems, including that of the ARTIS Pheno. More recently, a new EFOMP protocol [2] was introduced to guide dynamic X-ray system testing. The Siemens ADRC optimizes exposure settings in real-time using a Signal Difference to Noise Ratio (SDNR) approach with spatial frequency weighting [3]. As a standard detector-dose-driven ADRC, it dynamically adjusts tube voltage, tube current, pre-filter, exposure time (pulse width), and focal spot to optimize the balance between dose and image quality. Additionally, the ARTIS Pheno considers object composition, size, and velocity [3]—an approach further evaluated in recent studies [4].

In this work, an alternative method for verifying detector linearity is explored by using "For Presentation" images instead of "For Processing" ones, typically not provided by the manufacturer due to the proprietary nature of the post-processing logic. This method assesses noise levels through background standard deviation analysis instead of the mean pixel values [2].

In conclusion, radiation dose monitoring and control are essential for ensuring patient safety and operator protection, minimizing exposure while maintaining high image quality. This is overseen by the medical physicist, verified during acceptance testing, and monitored through periodic quality controls. This study evaluates how the Siemens SDNR-based ADRC system impacts on exposure dose levels and whether detector quality control can be effectively assessed using "For Presentation" images.

[1] P.-J. P. Lin, et al., AAPM Report No. **125** (2012).
[2] EFOMP Protocol: "Quality control of dynamic X-ray imaging systems" (2024).
[3] M. Dehairs, et al., Phys. Med. Biol. **64** 045001 (2019).
[4] T. Werncke, et al., Med. Phys. **48** 7641 (2021).

T41

Impact of CT image data characterization on the absorbed dose calculation

M. Tolo [1], Đ. Smilović Radojčić [1,2], Nevena Obajdin[1,2] and S. Jurković [1,2]

[1]Medical Physics and Radiation Protection Department, University Hospital Rijeka, Rijeka, Croatia

[2] Department of Medical Physics and Biophysics, Faculty of Medicine, University of Rijeka, Rijeka, Croatia

The accuracy of determining the absorbed dose distribution in radiation oncology is highly dependent on the characterization of tissue image data. Therefore, calculation algorithms of commercial treatment planning systems require determination of the CT to Relative Electron Density (RED) or CT to Mass Density (MD) curve. Various parameters may affect the reading of the CT numbers e.g., tube voltage, reconstruction algorithm, the processing filters, etc. The aim of this study is to investigate the effect of different inherent CT system parameters on the absorbed dose calculation.

Study is divided in two parts. The first part is investigation of the impact of variation of the CT system (Siemens Somatom go.Open Pro CT simulator) parameters to determine the CT numbers. Therefore, the tube voltage was varied (70-140 kV, 10 kV step). Also, different clinical radiotherapy protocols (head, head and neck, breast, thorax, pelvic), and different reconstruction algorithms (five different levels of SAFIRE and iMAR) were used. A CIRS Electron Density Phantom with 16 inserts of known relative electron densities (0.003 to 12475) and mass densities (0.001 to 4.51 g/cm^3) was used to generate CTtoRED/MD curves. In the second part, the impact of chosen CTtoRED/MD curve on the calculated absorbed dose was investigated. Ten patients were selected for each radiotherapy protocol, fifty in total, and the planning techniques were forward IMRT (field-in-field) or VMAT. Patients' image data were acquired with a tube voltage of 120 kV, and the absorbed dose distribution was determined using a CTtoRED/MD curve averaged from each radiotherapy protocol data (120kV-average). For research purposes, four additional CTtoRED/MD curves (70kV-1, 70kV-2, 140kV-1, 140kV-2) were used to calculate the absorbed dose distribution using the AAA and Acuros XB calculation algorithms (Varian Eclipse) with absorbed dose reported as dose-to-medium and dose-to-water, respectively. For each image data set, ten points were selected for the absorbed dose comparisons, five within the target volume and five in the OARs.

A statistically significant difference in the CT number values was found between the different tube voltages and between two groups of radiotherapy protocols (head, head and neck versus chest, thorax and pelvis). There is no statistically significant difference in the CT numbers for different reconstruction algorithms used.

Regarding the difference of the calculated absorbed dose for different CTtoRED/MD curves, the difference for the AAA was less than 1% for all observed points. For the AcurosXB, the difference of more than 2.5% is observed for points with higher RED/MD (e.g., mandible) for both dose reports.

[1] M.W. Geurts, et al. J Appl Clin Med Phys. 23; 13641 (2022). DOI: 10.1002/acm2.13641

[2] M.B. Afifi, et al. J Rad Res Appl Sci. **17**, 100997 (2024). DOI: 10.1016/j.jrras.2024.100997

T42

Automated VBQ determination from T1-weighted lumbar spine MRI data using a hybrid CNN-Transformer neural network

Kristian Stojšić [1] , **Slaven Jurković** [1,2]

[1] *University Hospital Rijeka, Medical Physics and Radiation Protection Department, Rijeka, Croatia;*
[2] *Faculty of Medicine, University of Rijeka, Department of Medical Physics and Biophysics, Rijeka, Croatia;*

The vertebral bone quality (VBQ) score is a new scoring method in magnetic resonance imaging (MRI) that can be used to enhance the screening for osteoporosis [1]. The aim of this research is to provide a method of automatic VBQ determination from T1-weighted sagittal lumbar spine MRI images using segmentation obtained with a trained neural network model and to compare different methods of vertebrae and cerebral spinal fluid (CSF) ROI post-processing.

BRAU-Net++ neural network architecture was chosen for the segmentation task of 9 classes (8 vertebrae and the spinal canal) required for automatic VBQ determination. This u-shaped architecture is a hybrid CNN-transformer network that uses bi-level routing attention (BRA) as the core building block for its encoder-decoder structure [2]. A large publicly available dataset of 447 sagittal T1 and T2 MRI series, with their corresponding ground truth segmentation masks, was used to train the neural network after several pre-processing steps [3]. To evaluate the performance of the neural network, the average Dice-Similarity Coefficient (DSC) was used, along with precision and accuracy. Four different methods of automatic VBQ determination with different approaches to vertebrae and CSF ROI post-processing were explored. Two of the methods use T1-weighted, while the other two use T2-weighted images for CSF ROI selection with a connected threshold algorithm. Another dataset consisting of 83 T1-weighted and 83 T2-weighted lumbar spine MRI data was chosen at random from the resident hospital database to evaluate the statistical significance of different VBQ determination methods using one-way ANOVA statistics.

The neural network achieved convergence and produced a trained model that was later used to generate segmentations of vertebrae and spinal canal. The resulting model achieved good accuracy, precision, and DSC scores. The results of one-way ANOVA statistical analysis show that there are statistically significant differences between methods using T1-weighted, and methods using T2-weighted images for generation of segmentation masks.

Automatic VBQ determination was successfully achieved by using the segmentations from the trained neural network model with the addition of analytical CSF segmentation using a connected threshold algorithm. Automatization of the segmentation process opens new possibilities for bone quality assessment, such as further improving the VBQ score results by removing regions of hyperintense signal or enhancing the bone quality determination using new methods.

[1] Ehresman, J., Pennington, Z., et.al. Novel MRI-based score for assessment of bone density in operative spine patients. Spine J. (2020) doi: 10.1016/j.spinee.2019.10.018.

[2] Lan, L., Cai, P., et.al., Y. BRAU-Net++: U-Shaped Hybrid CNN-Transformer Network for Medical Image Segmentation. arXiv preprint (2024) doi: 10.48550/arXiv.2401.00722

[3] van der Graaf, J.W., van Hooff, M.L., Buckens, C.F.M. et al. Lumbar spine segmentation in MR images: a dataset and a public benchmark. Sci Data 11, 264 (2024) doi: 10.1038/s41597-024-03090-w

T43

GEANT4 BASED SIMULATION OF THE GAMMAPOD™ SYSTEM

M.I. Subia[1], F. Longo[1], E. Moretti[2], P. Scalchi[2]

[1] *Università di Trieste, Dipartimento di Fisica, Trieste, Italy*
[2] *ASU FC, SOC Fisica Sanitaria, Udine, Italy*

The GammaPod™ (GP) (Xcision) is a stereotactic radiotherapy device for breast cancer, utilizing 25 Co-60 sources arranged in a hemisphere to dynamically deliver dose via non-overlapping rotating beams. A co-rotating concentric collimator hemisphere provides 15-mm and 25-mm field sizes at the isocenter. The system allows for same-day treatment, with the breast immobilized throughout imaging and therapy. Since single-fraction delivery occurs immediately after simulation CT, dose verification measurements are performed afterward. However, to ensure treatment accuracy prior to delivery, routine patient-specific quality assurance (PSQA) requires independent dose calculations. Despite the existence of such dose calculation engines [1,2], no commercially available independent second-check software currently exists for the GP. As a result, the development of a Monte Carlo (MC)-based calculation algorithm is highly recommended during clinical use.

Based on the logic of the Geant-4 Gammaknife Advanced Example [3], the main components of the GP unit were simulated: the cylindrical Co-60 sources, the collimation system, a PMMA breast phantom used for dose calibration and absolute dose-rate measurements (with its corresponding cylindrical scoring mesh simulating the RAZOR chamber (IBA) sensitive volume) , and the SRS MapCheck phantom (Sun Nuclear) used for dose relative measurements (with a rectangular planar mesh). Rotation of the GP system was simulated by rotating the scoring mesh.

Simulations were validated both qualitatively and quantitatively, confirming correct source positioning, energy distribution, and collimation. The model reproduced experimental dose-rate measurements for fixed collimators with an absolute difference of <7%. Additionally, the penumbra reduction effect observed in rotating gamma systems [4] was tested.
Results suggest that a Geant4-based independent dose calculation tool for GP is technically feasible. Future work will assess computational requirements for full clinical treatments simulations.

[1] W. Lu, et al., Independent Dose Calculation for GammaPod Treatment, AAPM Annual Meeting (2019).
[2] Becker, S. et al., Development and validation of a comprehensive patient-specific quality assurance program for a novel stereotactic radiation delivery system for breast lesions. Journal of applied clinical medical physics (2019)
[3] F. Romano et al., Geant4-based Monte Carlo Simulation of the Leksell Gamma Knife, IEEE Nuclear Science Symposium Conference Record (2007)
[4] Cheung JY, Yu KN. Rotating and static sources for gamma knife radiosurgery systems: Monte Carlo studies. Med Phys. (2006)

T44

SECURE project – Recommendations for minimization of radiation exposure in the isotope chain

G de With[1], E. Winters [1], G.W. Sandker[1] and P. Tomše [2]

[1]NRG PALLAS – Consultancy & Services, Arnhem, The Netherlands
[2] University Medical Centre Ljubljana, Slovenia

Introduction: Strengthening the European Chain of sUpply for next generation medical RadionuclidEs (SECURE) project of European Nuclear Education Network (ENEN) aims to make a major contribution to the sustainability of medical isotope production and its safe application. α-emitting isotopes coupled to highly target-specific molecules are widely investigated for use in targeted alpha therapy (TAT). Clinical results show these are potent targeted drugs and a great potential in cancer therapy. Nevertheless, adequate consideration of radiation protection measures is required. Therefore, we developed a radiological benchmark tool which considers exposure scenarios that cover the full isotope chain.

Materials and methods: Three specific radiation protection issues were considered. (1) To determine the radiation doses for workers, caregivers and public involved throughout the lifecycle of the TAT-isotope, considering relevant exposures, pathways and radionuclide inventories. (2) To make a comparison of the radiation doses from the exposure scenarios for the different TAT-isotopes and their production routes. (3) To perform an analysis on the computational findings from the radiological benchmark and extract lessons learned, draw recommendations for best practice, and identify areas and topics that require attention from a radiation protection perspective.

Results: The benchmark tool was designed to assess radiation exposure through all possible exposure routes (external radiation, inhalation, submersion, and ingestion) and calculate the effective doses as well as equivalent doses for the eye, extremities and skin.
The isotope's life cycle is divided into the following stages: production, purification, labelling and clinical practice. Each stage is covered by scenarios with defined time line, distribution factor, mode of chemical processing, exposure time, shielding, distance, and indoor and outdoor exposure parameters. The nuclide inventory is computed for each scenario and forwarded to the next scenario considering any chemical processing, discharges, waste, or dissemination to multiple users.
The process of decay and in-growth for a network of radionuclides is described considering initial activities, decay rates and complex decay chains including multiple decay branches.
The results from the benchmark tool demonstrate that choices made in the design of the isotope production process strongly impact potential radiation risk, waste generation, and effective use of infrastructure and source material. Furthermore, recommendations on the safe use should be tailored to the specific radiological needs of the TAT-isotope in question.

Summary: We developed a radiological benchmark tool which clearly indicates considerable variation in radiation dose for the various TAT-isotopes along its life cycle with strong variation in the relative contributions from different exposure routes. Insights can be obtained that help to improve radiation protection issues involving α-emitting isotopes.

T45

CT imaging through combined source- and detector-generated spectral separation

Stevan Vrbaški[1,2,3], **Adriano Contillo**[2], **and Renata Longo**[2,3]

[1] *University of Novi Sad, Faculty of Medicine, Hajduk Veljkova 1-3, 21000 Novi Sad, Serbia*

[2] *Elettra-Sincrotrone Trieste S.C.p.A, 34149 Basovizza Trieste, Italy*

[3] *Department of Physics, University of Trieste, Via Valerio 2, 34127 Trieste, Italy*

Spectral computed tomography (CT) is utilized in clinical imaging to obtain virtual monochromatic images, tissue density, and effective atomic number maps [1]. Two spectral channels are just as effective as multiple spectral channels for these tasks, with the quality primarily dependent on the spectral separation of the independent channels [2]. Clinical spectral CT scanners achieve spectral separation using either dual-energy spectra or spectral detectors, such as dual-layer or photon-counting detectors.

This work has developed an approach to test the impact of spectral separation on relevant clinical tasks using the combined contribution of source-generated and detector-generated spectral separation in CT imaging. The setup was made using synchrotron radiation at SYRMEP beamline at Elettra Synchrotrone Trieste, where the polychromatic synchrotron X-ray source is spectrally shaped using a foil made of pure silver. The spectral separation on the detector side was obtained using a two-threshold photon-counting detector

Preliminary results show that this method can obtain quantitatively correct virtual monochromatic images of tissue-equivalent inserts and estimate their density and effective atomic number. The results were validated using CT images acquired with a synchrotron beam filtered by a double-crystal monochromator (true monochromatic images) and ground truth data. The experimental setup is given in Figure 1.

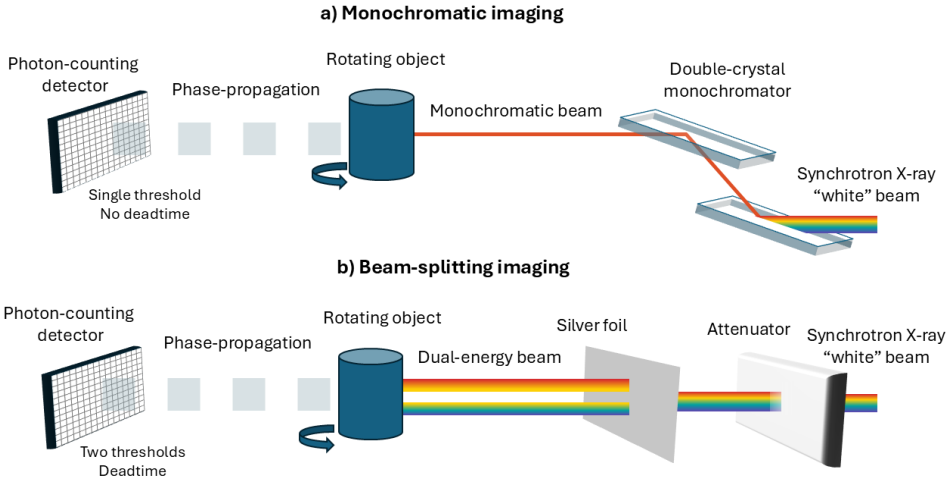

Figure 1: Comparison of conventional, monochromatic imaging approach and beam-splitting technique introduced in this paper.

[1] M. H. Albrecht, T. J. Vogl, Radiology, **2**, 293, (2019).
[2] S. Vrbaski, R. Longo, and A. Contillo. SPIE, 12031 (2022).

T46

Evaluation of an almost-autonomous dosimetric workflow for the management of laryngeal cancer in radiotherapy

Moritz Westermayer[1,2,3], Daniela Sandu[1], Cécile Laude[1], Séverine Racadot[1], Vincent Grégoire[1] Anne-Agathe Serre[1], David Sarrut[2], Marie-Claude Biston[1,2]

[1] Centre Léon Bérard, 28 rue Laennec 69373 LYON Cedex 08 - France

[2] CREATIS, CNRS UMR5220, Inserm U1044, INSA-Lyon, Université Lyon 1, Villeurbanne - France,

[3]Therapanacea, 75004 Paris, France

Background and purpose: In radiotherapy, numerous studies have demonstrated the individual performance of autosegmentation and autoplanning solutions in saving time and in reducing the inter-operator-variability (IOV) with the aim of harmonizing the treatment plan quality [1-2]. However, the feasibility of an entirely autonomous workflow was rarely investigated. Taking into perspective the IOV in CTVn delineation, we evaluated the feasibility of an almost-automatic dosimetric workflow for the management of laryngeal cancer using a commercial Deep Learning (DL) autocontouring solution (ART-Plan Annotate, TheraPanacea) and a preclinical version of autoplanning solution based on a priori multicriteria-optimization (MCO) algorithm (mCyle, Elekta).

Material and Methods: Ten non-operated head-and-neck cancer patients previously treated in VMAT were selected. Target contours of the clinical plans were manually delineated by an expert physician, whereas organs-at-risk (OARs) were automatically contoured, and corrected. OARs and clinical target volumes (CTVn) were retrospectively delineated automatically, with macroscopic tumor volumes copied from clinical plans, and automatic plans generated. Then CTVn levels were manually delineated by 4 other physicians. The IOV in CTVn delineation and the variability in experts' contours towards autocontours was quantified using geometric metrics (dice (DSC); surface DSC; 95th percentile-Hausdorff distance ($HD_{95\%}$)). Dose differences between auto- and clinical plans calculated on the clinical contours were quantified. The dosimetric effect of IOV in CTVn delineation were evaluated on manual and autoplans.

Results: $HD_{95\%}$ and surface DICE results indicated significant differences across most physicians' contours ($p \leq 0.04$). Significant difference between IOV and MAV across all metrics was found ($p < 0.001$). Automatic plans optimized on uncorrected autocontours generally resulted in better OARs' sparing while providing a higher PTVn coverage. The impact of the IOV on PTVn coverage was found to be amplified on autoplans with an increased inter-quartile-range by 42.8%.

Conclusion: Deep Learning autocontouring provided a higher consistency in CTVn contours and highly accurate OARs-delineation. Superior treatment plans quality was provided by fully automated workflow. However, this came at the expense of an increased difference in PTV coverage due to IOV.

[1] Vandewinckele, L. et al. Overview of artificial intelligence-based applications in radiotherapy: Recommendations for implementation and quality assurance. Radiotherapy and Oncology, 153, 55-66 (2020).

[2] Kosmin, M. et al. Rapid advances in auto-segmentation of organs at risk and target volumes in head and neck cancer. Radiotherapy and Oncology, 135, 130-140 (2019).

T47

Collimated Carbon ion beams for preclinical in-vivo research

L. Wolf [1,2], W. Ikegami Andersson[3], L. Glimelius[3], D. Georg [1,2] and B. Knäusl[1,2]

[1] Division of Medical Physics, Department of Radiation Oncology, Medical University of Vienna, Vienna, Austria
[2] MedAustron Ion Beam Therapy Centre, Wiener Neustadt, Austria
[3] RaySearch Laboratories, Stockholm, Sweden

Preclinical research is a cornerstone of radiation oncology, encompassing a broad spectrum of methods ranging from in vitro experiments to more clinically relevant in vivo models. In recent years, interest in preclinical studies within particle therapy has grown. [1,2] In vivo studies investigating radiation-induced side effects and tumor response in small animals require the highest accuracy and conformity in irradiation delivery, often necessitating beam collimation. However, standard infrastructure at particle therapy centres is typically insufficient to meet these requirements and established commercial clinical dose engines generally do not support collimated ion beams. This study aimed to further expand the available infrastructure and benchmark a prototype pencil beam dose engine (RaySearch Laboratories, Stockholm, Sweden) for collimated carbon ion beams.
Validation plans were optimized for Spread-Out Bragg Peaks (SOBPs) to cover targets with diameters of 3, 7, 12, and 31 mm and lengths of 3, 5, 10, and 30 mm at multiple depths. Beam collimation was achieved using a modular collimation system with interchangeable secondary collimators (diameters of 5, 10, 15, and 34 mm). [3] A microDiamond detector (PTW-Freiburg, Freiburg, Germany) was positioned at effective depths ranging from 1 to 25 mm within a 60 × 60 cm² RW3 phantom for depth dose measurements, which were used to benchmark the dose engine in terms of root mean square error (RMSE).
The RMSE for measurements with 5, 10, 15, and 34 mm apertures were 6%, 6%, 5%, and 3%, respectively, with better agreement observed for larger aperture diameters. While the TPS tended to underestimate the dose for the 5, 10, and 15 mm apertures, it overestimated the dose for the largest aperture (34 mm). The maximum deviation of −12% was observed for the smallest aperture, suggesting that beam spread due to scattering requires further refinement.
This study presents the first benchmarking results of a prototype pencil beam dose engine for collimated carbon ion beams in a preclinical setting. While agreement between measurements and calculations improves with larger collimators, deviations for smaller apertures highlight the need for further refinement. Future efforts will focus on optimizing the dose engine to improve accuracy in preclinical carbon ion treatment planning.

[1] B.F. Koontz *et al*., Br J Radiol. **90**, 1069 (2017), 10.1259/bjr.20160441
[2] M. Dosanjh *et al*., Radiother Oncol. **128**, 1 (2018), 10.1016/J.RADONC.2018.03.008
[3] B. Knäusl *et al*., Phys Med. **113**, 102659 (2023), 10.1016/j.ejmp.2023.102659

T48

Evaluating the impact of Diffusion Weighted Imaging for Gross Tumor Volume delineation in cervical carcinoma patients

Lukas Zimmermann[1], **Barbara Knäusl**[1], **Johannes Knoth**[1], **Alina Sturdza**[1], **Vincent Dick**[1], **Tatevik Mrva-Ghukasyan**[1] **and Maximilian Schmid**[1]

[1]*Department of Radiation Oncology, Christian Doppler Laboratory for Image and Knowledge Driven Precision Radiation Oncology, Medical University of Vienna, Vienna, Austria*

Introduction: The combination of radiochemotherapy and magnetic resonance imaging (MRI)-guided adaptive brachytherapy (BT) is the standard of care for locally advanced cervix carcinoma. The definition of adaptive gross tumor volume (GTV) with T2 weighted sequences is performed according to international guidelines [1], however, precise assessment of the shrinking residual tumor during radiotherapy is difficult, resulting in high inter-observer variation. Including a diffusion weighted imaging (DWI) sequence could potentially improve the delineation process. Therefore, the goal of this study was to evaluate the implication of the additional sequence on the inter-observer variability.

Methods: All patients with locally advanced cervical carcinoma treated between xx/2022 to xx/2024 with radiochemotherapy (25×1.8 Gy) followed by brachytherapy, were selected for this analysis [EC number: 1818/2024]. Inclusion criteria implied performance of MRI with DWI and T2w sequences (Philips Ingenia RT) with prospectively defined settings at three different time points: 1) at diagnosis (init), 2) before BT without applicator (preBT) and 3) at BT with applicator (BT). Five physicians (three experts and two beginners) delineated the GTV twice for each patient, once according to the guidelines on the T2w image alone and once with fused DWI. A consensus structure of all experts was generated using the STAPLE algorithm, which was considered the ground truth. The consistency over the volume delineation was assessed with volume comparisons and overlap measures (DICE, 95th hausdorff distance, Intersection over union (IoU)). We use the Wilcoxon Signed Rank test to check for statistical significance ($p < 0.05$).

Results: In total 27 patients were available. The delineated volume differed between DWI and T2w segmentation by 3.1/0.8/0.4 cm^3 (init/preBT/BT) showing consistently smaller structures on the DWI. DWI improved consistency between expert delineations for init (IoU +8% median) and BT (IoU +13% median) time points. Beginners improved significantly when considering DWI in the delineation process compared to the STAPLE structure at all time points. Correspondingly, Hausdorff distances with respect to the consensus structure were 2.7±1.2/4.0±2.7, 2.9±2.0/3.5±3.1 and 3.6±2.0/4.7±2.8 mm (to read as DWI/T2w median±IQR) for init, preBT, and BT, respectively.

Discussion:

Our study demonstrated the potential of DWI MR sequences to improve the consistency of GTV delineations in cervical cancer patients between experts and novices for various time points.

[1] International Commission on Radiation Units and Measurements. Prescribing, Recording, and Reporting Brachytherapy for Cancer of the Cervix (ICRU report 89). Bethesda: 2013.

T49

Dosimetry and tracking accuracy evaluation of lung carcinoma treated with **RADIXACT®**TREATMENT DELIVERY SYSTEM and Synchrony Real-Time Delivery Adaptation using Dynamic Thorax Phantom 008A and CIRS motion platform.

Ivona Zlatkova [1], Ferdinando Francomacaro [1,2]

[1]Emicenter [2] Emicenter

Purpose: To test the intrinsic geometric accuracy of the Synchrony Real-Time Delivery Adaptation for Radixact® TomoTherapy. System performance in adapting to target translations in left-right (LR) and inferior-superior (IS) directions for various amplitudes and breathing patterns was studied using 1 and 2.5cm jaw collimations and two spherical targets with diameter of 1 and 2cm.

Methods: A Dynamic Thorax Model 008A chest phantom with LAA-1259-1 insert, was used for this purpose. The entire setting was placed on the CIRS Motion Platform controlled by the CIRS Motion Control software® [2]. The Log Files generated by the Accuray Precision Software® and CIRS Motion Control files, with instructing coordinates prepared specifically for the tests were analysed. Phase shifts between the tumour motion and the respiratory Light Emission Diodes (LEDs) were introduced to evaluate the ability of Synchrony to respond to unsynchronized movements between the target and the relevant surrogate.

Results: The capabilities of the Synchrony system to track in real-time and adapt to target position were evaluated, for sinusoidal and shark wave functions. The Root Mean Square Error (RMSE) values between target position predicted with Synchrony and actual target position commanded with the CIRS Motion Control Software were calculated. The results show that a lateral movement of 0.5mm and amplitude of 19mm fails the verification by a factor of 1.8 above the limit of RMSE<1.5 for 1cm jaw collimation. For 2.5cm jaw collimation, Synchrony improved in performance, obtaining sub millimetric accuracy for IS amplitudes ≤1cm.

$$\mathrm{RMSE} = \sum_{i}^{n} \frac{\sqrt{X_m - X_c}}{N}$$

Trace with phase deviation of -0.4s with respect to LEDs movement had 0.63 times smaller RMSE compared to phase deviation of -0.8s (the target is behind the external surrogate), both with RMSE <1.5mm. The “Shark” motion was tracked in SYN modality within the tolerance limit for 137s of continuous tracking. The best tracking result with overall 0.44mm error for 220s tracking duration was calculated for the trace with no phase shift and no rotation applied. The absolute dose dosimetry test showed that a fiducial with 1.5cm offset during treatment was tracked successfully giving ±1.6% dose difference from the one calculated on the originally planned target position, for six consecutive tests.

Conclusions: Tumour motion due to breathing can follow complex trajectories, varying in phase shift, amplitude and oscillation pattern. Nonetheless, Synchrony was able to adapt to the target position within tolerance level, for all traces with 2.5cm jaw collimation used clinically for most of the stereotactic adaptive treatments for pulmonary targets.

[1] Mei Yan Tse, Wing Ki Claudia Chan, Tsz Ching Fok, Tin Lok Chiu, Siu Ki Yu. 23, 13600 (2022)

[2] Dynamic phantoms User guide. Image acquisition, treatment planning, dose delivery. Model 008A, 008A-20, 18023-A, 18043-A CIRS. www.cirsinc.com